Conceptual Design of Swept Wing Root Aerofoils

Marten Bralte Sol

Technische Universiteit Delft

TU Delft Delft University of Technology

Challenge the future

Conceptual Design of Swept Wing Root Aerofoils

by

Marten Bralte Sol

in partial fulfillment of the requirements for the degree of

Master of Science
in Aerospace Engineering

at the Delft University of Technology,
to be defended publicly on Friday August 21, 2015 at 13:00 PM.

Supervisor:	Dr.ir. Roelof Vos,	TU Delft
Thesis committee:	Prof.dr.-ing. Georg Eitelberg,	TU Delft
	Dr.ir. Sander van Zuijlen,	TU Delft
	Dr.ir. Roelof Vos,	TU Delft

An electronic version of this thesis is available at http://repository.tudelft.nl/.
Thesis registration number: 258#15#MT#SEAD-FPP

TU Delft Delft University of Technology

SUMMARY

For modern transonic transport aeroplanes, it is important to produce low drag at high cruise speeds. The root effect, caused by effects of symmetry on swept wings, decreases the performance of these aeroplanes. During aeroplane design, root modifications are applied to counteract this decrease in performance. Most conceptual aeroplane design tools do not have a method for design of the root aerofoil. However, the design of the root aerofoil has a significant influence on the properties of the final design, since it transfers the loads from the wing to the fuselage. Therefore, having a conceptual method for design of the wing root aerofoil will increase the accuracy of a conceptual aeroplane design. For conceptual design, computational times are important, to allow the designer to try different approaches and get a feel for the design. In this report a method is developed to approximate the root aerofoil design to achieve straight isobars on a wing of any given shape, within computational times that are suitable for conceptual design.

First a method is developed for estimating the pressure distribution over the root aerofoil of a given wing. This is done by combining a method for estimation of the root effect due to thickness, a method for estimation of the root effect due to lift, a Vortex Lattice Method (VLM) and a two-dimensional panel method. A full potential method, MATRICS-V, is used to verify the results of the method, because of its proven validity. It is shown that the results of the first part of the method are generally in good agreement with results found by MATRICS-V. The effects of wing sweep, wing taper and addition of a wing kink can be modelled with results that are in good agreement with the verification data. For aft swept wings with positive lift, the pressure near the leading edge is underestimated. For forward swept wings with positive lift, the pressure on the upper surface is overestimated. For wings with a cambered aerofoil an inaccuracy occurs over the forward part of the profile. The general shape of the curve, however, is captured.

Secondly, this method is coupled with an optimisation method for the root aerofoil, using Class-Shape function Transformation (CST) parametrisation. The target of the optimisation is set to achieve a similar pressure distribution over the wing root aerofoil as the pressure distribution over the outboard section of the wing.

For the developed method, it is difficult to show that the results are valid, since there is no method that has a one-to-one match with the method developed. Therefore, the results are compared to the general characteristics observed in actual root aerofoil designs. The method shows the characteristic behaviour in terms of change in camber, change in location of maximum thickness and change in incidence angle. The increase in thickness, however, is not present. This is caused by the fact that the lower surface pressure distribution is also set as a target. In actual aeroplane design the lower surface is of less importance. In the method developed, however, it is of importance to retain the shape of specific aerofoil designs, like supercritical aerofoils, during optimisation. As a final verification, an optimised root aerofoil design is analysed using MATRICS-V. The results show that the root section pressure distribution is in good agreement with the outboard pressure distribution. In terms of computational time, the method is shown to generally produce reliable results within 30 seconds.

ACKNOWLEDGEMENTS

The work presented in this thesis would not have been possible without the invaluable feedback, help and support of a number of people:

First of all, I would like to thank my supervisor, Dr.ir. Roelof Vos, for his guidance during this thesis. He has a way of making you take a good look at your results and think about what they mean. I would like to thank Dr. Ali Elham for his help setting up and running MATRICS-V. I would also like to thank the *Flight Performance and Propulsion* graduate students of room 6.01, for providing both a social, and a productive environment during the work on my thesis.

I would like to thank my parents for their unrelenting support through my years of study. Furthermore, I would like to thank my friends, without whom I would not be the person I am today. In particular my friends from high-school, Aerospace Engineering and from the student korfball club D.S.K.V. Paal Centraal.

Finally, I would like to thank my girlfriend, Elize, who never stopped supporting and encouraging me.

CONTENTS

List of Symbols

ϵ	Pressure coefficient error (~).
$\delta\epsilon_{\text{des}}$	Desired minimum change in error value for optimisation (~).
ϵ_{tot}	Total pressure coefficient error (~).
Λ	Wing sweep angle, quarter chord unless specified (rad).
λ	Taper ratio (~).
θ	Constant angle for cosine distribution (rad).
A	Wing aspect ratio, b^2/S (~).
a_0	Lift slope coefficient of two-dimensional aerofoil (1/rad).
b	Wing span (m).
c	Chord length (m).
c_{l}	Section lift coefficient (~).
C_{p}	Pressure coefficient (~).
δc_{l}	Change in section lift coefficient (~).
ΔC_{p}	Pressure differential, $C_{p,\text{upper}}$ - $C_{p,\text{lower}}$ (~).
δC_{p}	Change in pressure coefficient C_p (~).
$f(\Lambda)$	Source strength term, root effect due to thickness (~).
k	Interpolation function for shift in aerodynamic centre (~).
M_{dd}	Drag divergence Mach number (~).
n	Number of chordwise points (~).
S_1	Approximate expression developed by Multhopp (~).
S_2	Approximate expression developed by Multhopp (~).
t	Shape parameter (~).
V	Particle velocity (m/s).
V_{e}	Flow component perpendicular to the swept wing (m/s).
V_∞	Free-stream particle velocity (m/s).
V_{par}	Flow component parallel to the swept wing (m/s).
y_{c}	y Co-ordinate in terms of chord length (~).
y_{kink}	Spanwise position of the wing kink (m).
y_{pos}	spanwise fraction from root to tip (~).

List of Abbreviations

AVL	Athena Vortex Lattice.
CDF	Computational Fluid Dynamics.
CST	Class-Shape function Transformation.
MDO	Multidisciplinary Design Optimization.
NACA	National Advisory Committee for Aeronautics.
NASA	National Aeronautics and Space Administration.
NLR	National Aerospace Laboratory.
RAE	Royal Aircraft Establishment.
VLM	Vortex Lattice Method.

1

INTRODUCTION

Aeroplane design is a competitive business where margins are small. In this competitive environment, companies strive for the highest possible fuel efficiency. This urge for lower fuel consumption drives designs to achieve higher speeds, reducing the time in the air and thereby the fuel used. At a certain threshold, however, an increase in speed results in an exponentially large increase in drag. Flying at speeds above this threshold actually reduces fuel efficiency. This threshold is called the drag divergence Mach number (M_{dd}) [1].

Wing design for modern transonic transport aeroplanes is driven to produce the required amount of lift, while producing a minimum amount of drag at a M_{dd} that is as high as possible. In order to achieve a high M_{dd}, it is important that local supervelocities on the surface of the wing do not surpass that of other parts of the wing. This would result in local early shock formation, resulting in increased drag. At the wing root of an aft swept wing, the so-called 'root effects' influence the flow in such a way that the velocities over the leading edge part of the aerofoil are lower while velocities over the trailing edge part are higher. Because of the curvature of the aerofoil this results in pressure drag near the root [1].

The combined effects of not surpassing velocities of the other parts of the wing and not having lower velocities on the forward part and higher velocities at the aft part, near the root, set a clear goal for root aerofoil design. This is to produce a pressure distribution that as similar as possible to that of the outboard section of the wing. Another way of describing this is designing for straight isobars along the span.

Most conceptual design methods don't have a method for designing the wing root. Instead, the same aerofoil is used throughout the wing. The design of the wing root aerofoil has a significant influence on the properties of the final design, since it transfers the loads from the fuselage to the wing. Having a thicker wing is beneficial to wing weight since a larger area is available to support the wing bending moment [2].

Having a more accurate wing root design during the conceptual phase, serves two purposes. For industrial purposes, having a more accurate conceptual design might avoid costly changes in later stages of the design. For academic purposes, aeroplane conceptual design studies are often used to investigate new technologies. Having a more accurate conceptual design will improve the accuracy of these technology studies.

There are methods available for designing a wing with straight isobars across the span using a full wing Multidisciplinary Design Optimization (MDO) [3]. These methods take several hours of computational time. Conceptual design, however, requires computational times that are significantly lower. During conceptual design it is important that the designer can quickly try different options, to get a feel for his design.

Therefore, in this report a method is developed to approximate the root aerofoil design to achieve straight isobars on a wing of any given shape, within computational times that are suitable for conceptual design.

To this end, Chapter 2 explains the theory behind conceptual wing root design. In Chapter 3, two methods are found for estimating the two parts of the root effect. Using these methods, in Chapter 4 an estimation method is developed for the pressure distribution over the root section. In Chapter 5, this method is coupled with an optimisation routine to develop a method for designing root aerofoils for achieving straight isobars. The conclusions are shown in Chapter 6 and the recommendations in Chapter 7.

2

Wing Root Design

When investigating the conceptual design of swept wing root aerofoils, it is important to understand the framework of such a design. To this end, the conceptual design phase of an aeroplane is explained in Section 2.1. Section 2.2 shows the typical process of wing design during this conceptual phase. The so-called 'root and tip effects' will be explained in Section 2.3. The influence of these effects on design of the wing root is shown in section 2.4. Typical results of wing root designs in practice are shown and discussed in Section 2.5. Combining all the information in this chapter a research objective is developed in Section 2.6.

2.1 Conceptual Design Phase

The design of an aeroplane can be divided into three phases; conceptual design, preliminary design and detail design. During conceptual design the basic configuration, size and weight are determined, along with the initial performance. If these results look promising in terms of a technical design as well as in terms of market prospect, the design could be developed further. Usually, a number of conceptual designs are compared after which the best option is selected. During the preliminary design phase, the chosen design is developed further. Modifications are made continuously until the design is frozen. This marks the end of the preliminary design phase. At this point the decision has to be made whether or not to develop the aeroplane. This is also jokingly referred to as "you-bet-your-company". If the go-ahead is given, the aeroplane enters the detail design phase. In this phase all the actual parts to be built are designed. Also, the test and manufacturing methods are developed. After delivery of the first aeroplane, development will continue in the form of minor improvements and developing stretched versions of the aeroplane [4, 5].

In this report, the focus is on conceptual design. As explained above, during the conceptual design phase the designers want to be able to compare different designs. Therefore, it is important to use design methods that have a low computational time. This way, the designer can quickly try different approaches and get a 'feel' for the design.

The method developed during this thesis is to be implemented into a conceptual aeroplane design tool called the *Aircraft Initiator*. This design tool, of which the basics are explained in reference [6], uses an iterative process to find an optimal conceptual aeroplane design based on a number of top level requirements. The tool is of an iterative nature, meaning that calculations are repeated until a satisfactory result is found. This puts even more emphasis on the importance of low computational time.

2.2 Conceptual Wing Design

The first step of a new wing design is the design of the wing planform. The planform design is based on empirical data. This data can be obtained from conceptual design book methods like the one developed by Roskam, shown in Section reference [7], but for aeroplane manufacturers the starting point is usually design experience from earlier designs. This data is then used to generate a two-dimensional top down design of the wing. Important choices in this phase are the wing sweep angle, aspect ratio and taper ratio. Another important parameter that needs to be selected is the thickness to chord ratio. Something else that is commonly seen on transonic transport aeroplanes is the so-called 'wing kink'. It is an extension of the wing near the root resulting in a straight trailing edge. It is usually added to house the landing gear.

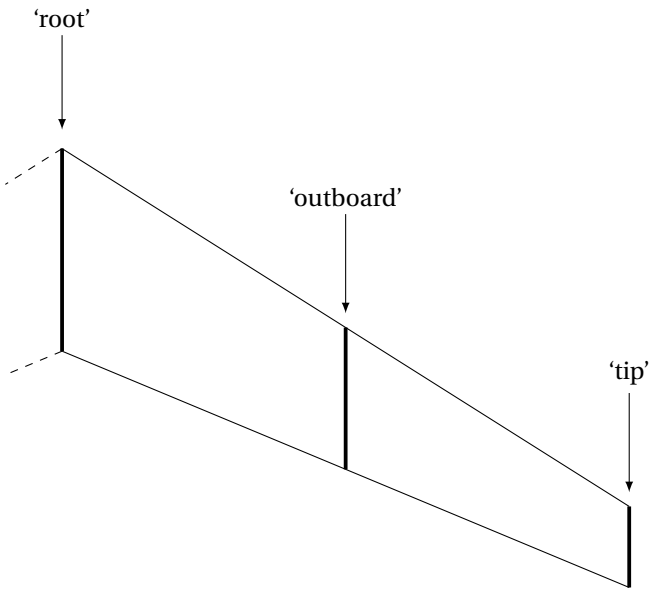

Figure 2.1: Definitions used for positions on the wing.

The second step is selection of the base aerofoil. This is mostly dependent on aeroplane cruise conditions. The design aim of an aerofoil is to develop the required amount of lift, produce a low amount of drag for the given thickness to chord ratio, fly at the desired cruise speed and achieve this with attached flow. For modern transport aeroplanes, flying in transonic conditions, the drag divergence Mach number (M_{dd}) is important. The drag divergence Mach number is the flight speed at which the drag starts increasing exponentially with speed. A high M_{dd} allows aeroplanes to fly faster without a severe penalty in drag, thereby increasing fuel efficiency. Most modern transport aeroplanes make use of the so-called 'supercritical' aerofoils. These aerofoils generate for a large region of flow slightly above Mach 1, terminated by a small shock wave. Towards the trailing edge the thickness is reduced and curvature is increased, causing more load to be carried by the aft part of the aerofoil, known as 'rear loading' [1].

Selection of the base aerofoil usually concludes the conceptual design phase. Therefore, most conceptual aeroplane designs do not have a specific wing root design, but rather place the same outboard aerofoil at the wing root.

With the 'outboard' section, the section at the centre of the semi-span is meant. This section is assumed not to be influenced by the root and tip effects, as will be explained in the next section. In order to give a clear overview of the definitions of the positions on the wing, these positions are shown in Figure 2.1.

2.3 ROOT AND TIP EFFECTS

The flow over an infinitely sheared wing can be separated into two components; the effective velocity V_e, perpendicular to the wing, and the parallel velocity V_{par}. Only the flow component perpendicular to the sheared wing is effected by the curvature of the wing surface. Since the flow component parallel to the swept wing, V_{par}, does not experience any curvature, it does not contribute to the pressure distribution. Therefore, on an infinitely sheared wing, the isobars are perpendicular to the direction of change of velocity and therefore straight and oriented along the span [1].

For a finite sheared wing, however, the situation is different near the plane of symmetry. At a plane of symmetry, both sides have the same properties. This makes it physically impossible to have a flow from one side to the other. This also makes it impossible for the flow component perpendicular to the direction of sweep, to 'sense' a curvature through the plane of symmetry. Because there is no curvature through the plane of symmetry, the only curvature experienced by the flow is along the line of symmetry. Therefore, the isobars, which are perpendicular to the direction of change of velocity, have to cross the plane of symmetry at a 90° angle. This is shown as curvature of the isobars near the plane of symmetry. The same effect can be seen at the wing tip, because the curvature of the wing does not continue past the wing tip. A typical isobar pattern of a finite swept wing can be seen in Figure 2.2, where the dashed lines indicate the straight isobar pattern of an infinite wing.

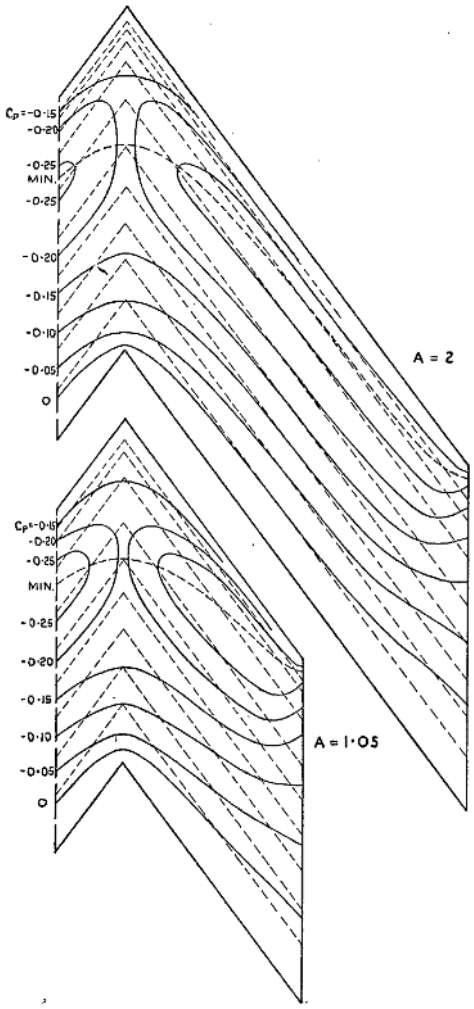

Figure 2.2: Isobars on two 53-deg swept-back wings of different aspect ratios [8].

For an aft swept wing, the effect near the plane of symmetry, or 'root effect', influences the flow in such a way that local velocities are lower near the leading edge part, when compared to an infinite wing. Near the trailing edge part, local velocities are higher. Because of this, the pressure near the leading edge part is higher, when compared to an infinite wing and the pressure near the trailing edge part is lower. Near the wing tip the effect, or 'tip effect', is reversed, with lower pressure near the leading edge and higher pressure near the trailing edge. For a forward swept wing both root and tip effects are reversed compared to the aft swept wing. The root and tip effects can be separated into two parts; a part caused by thickness and a part caused by lift [1].

In the direction of the span three regions can be defined with different properties. A region near the root, where the isobars curve to cross the plane of symmetry at a 90° angle, an outboard section where the flow properties can be approximated using simple sweep theory and a region near the tip where the isobars curve to leave the wing tip at an angle perpendicular to the flow. Küchemann et Al. state that the regions near the tip are no larger than one chord length from the root and tip, resulting in three separate regions for wings with an aspect ratio of larger than 2 [8]. Torenbeek states that the characteristics of part of the wing between 30-80% semi-span is obtained from simple sweep theory [4].

2.4 DESIGN FOR STRAIGHT ISOBARS

When designing a wing to take the root and tip effects into account, two things are of importance. First of all, wing design for modern transonic transport aeroplanes is driven to produce the required amount of lift, while producing a minimum amount of drag, at a M_{dd} that is as high as possible. In order to achieve a high

M_{dd}, it is important that local supervelocities on the surface of the wing do not surpass that of other parts of the wing. This would result in local early shock formations, resulting in increased drag.

Secondly, due to the curvature of the profile, pressures on the leading and trailing edge parts of the wing also generate a force in the streamwise direction. A low pressure near the trailing edge of a wing generates a force in aft direction called form or pressure drag. Since this drag reduces the aeroplanes performance, it is to be minimised [1].

The combined effects of not surpassing velocities of the other parts of the wing and not having increased form drag, sets a clear goal for spanwise aerofoil design. This is to produce a pressure distribution that is as similar as possible to that of the outboard section of the wing. Another way of describing this is designing for straight isobars along the span.

The thickness part of the root effect of a forward swept wing can be decreased by increasing thickness at the forward part and decreasing thickness at the rear part of the root. The lift part of the root effect can be decreased by decreasing camber or introducing negative camber. The resulting loss in lift can be compensated by increasing incidence. In order to obtain an elliptical lift distribution on a tapered wing with reduced root effect, the increase in thickness needs to be applied at the bottom. Root modification should blend in to the basic wing shape at about 30-40% semi-span [1].

Küchemann et Al. state that it is possible to calculate the pressure distribution, including root effect, over the root section of a swept wing. These calculations can also be used to modify the root section of a wing with a uniform aerofoil to achieve nearly straight isobars. This method might result in invalid aerofoils that intersect themselves. This means that the designed lower surface crosses the designed upper surface, creating an invalid shape. Extra care must be taken to avoid this problem. It could be that there is no aerofoil possible to create straight isobars [8].

2.5 EXAMPLE DESIGNS

In order to show that the theory explained in the past sections, an example of a real aeroplane wing root design is shown. The top of Figure 2.3 shows the outboard and root profiles of the Airbus A310 aeroplane. The bottom half of the figure shows the wing planform geometry. When looking at the root aerofoil of the A310, a number of things can be observed. First of all, it can clearly be seen that the overall thickness of the root aerofoil is larger than that of the outboard aerofoil. Also, the thickness near the leading edge shows a relativly high increase compared to the rest of the wing. Another noticable change is the decrease of camber. The incidence angle is not shown in the picture, but it shows an increase of about 5°.

In the book of Obert, a list is given of the modifications made to the outboard aerofoil for the design of a root aerofoil to obtain straight isobars. This list is shown in Table 2.1. The modifications shown in this list are in agreement with the findings on the A310 wing root design.

Mod. No	Modification	Reason
1	Increase the thickness of the forward part of the root section. Decrease the thickness of the rear part of the root section.	To obtain similar chordwise uppersurface velocity distributions due to thickness along the span.
2	Increase the thickness-chord ratio of the root section.	To obtain identical chordwise uppersurface velocity distributions due to thickness along the span.
3	Decrease the positive camber or apply negative camber on the root section.	To adapt the pattern of the chordwise uppersurface velocity distribution due to lift to that of the basic airfoil section.
4	Increase the incidence of the root section.	To obtain identical chordwise uppersurface velocity distributions along the span.

Table 2.1: List of root aerofoil design modifications to obtain straight isobars on an aft swept wing [1].

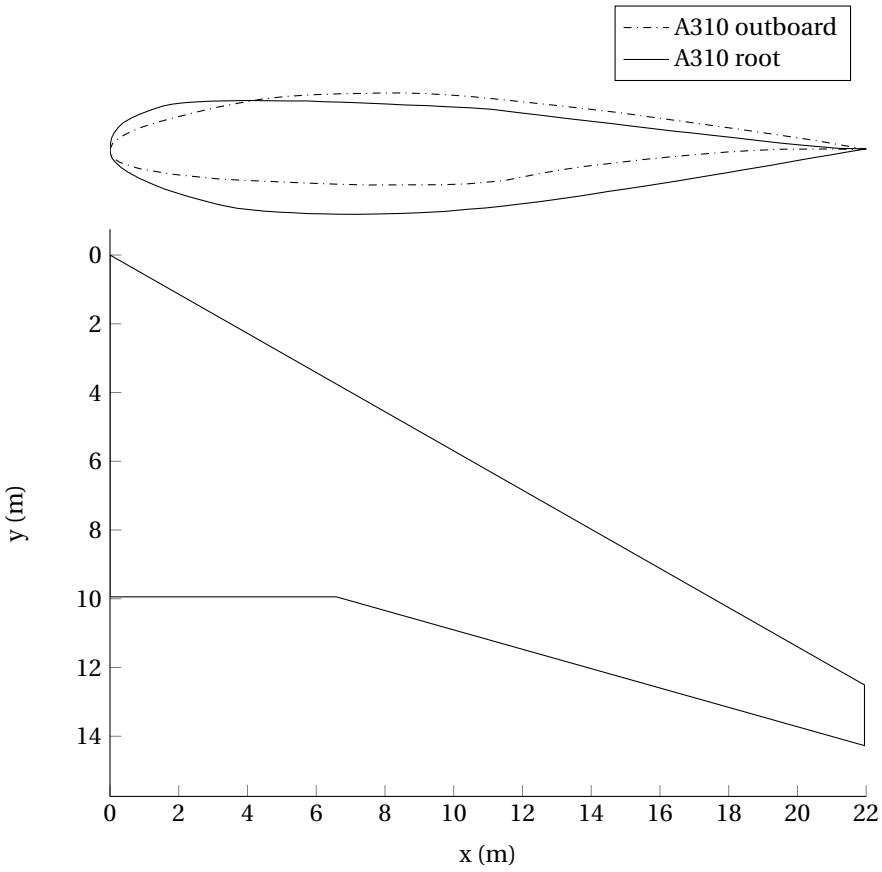

Figure 2.3: Wing root design of the Airbus A310 aeroplane [1].

2.6 RESEARCH OBJECTIVE

In Sections 2.1 and 2.2 the nature of conceptual aeroplane wing design is explained. It also shows the need for low computational times during this design phase. Section 2.3 explains the root and tip effects and Section 2.4 shows what is needed to incorporate these effects into the design of a wing.

Using these considerations, the objective of this thesis is described as:

> *"To develop a method to approximate root aerofoil design to achieve straight isobars on a wing of any given shape, within computational times that are suitable for conceptual design."*

3

Estimation of Root Effect

In order to develop a method for modelling the root aerofoil shape, the root effect needs to be estimated. This chapter describes two methods for estimating the root effect. The first method, shown in Section 3.1, shows the root effect due to thickness. The second method, shown in Section 3.2 shows the root effect due to lift. Both sections also evaluate the accuracy of the model shown.

3.1 Root Effect Due to Thickness

The 'Root and Tip effects' consist of two parts, as described in Section 2.3, a part that can be attributed to thickness and a part that can be attributed to lift. This section describes a method to estimate the part attributed to thickness. The estimation described is based on the methods by Küchemann and Weber in their report titled "The Subsonic Flow Past Swept Wings at Zero Lift Without and With Body", shown in reference [8].

The method and its application is explained in Section 3.1.1. In order to evaluate the accuracy of the method, MATRICS-V is used. A description of MATRICS-V can be found in Section 3.1.2. In Section 3.1.3 the method results are compared with data to show its validity. Finally, Section 3.1.4 explains the way lift is handled in the method.

3.1.1 Küchemann Weber Method

The method developed by Küchemann and Weber is a panel method in which the aerofoil is represented by a series of source filaments placed along the chord. In this method, the integrals of the panel method are replaced by a summation over a finite number of points. These summations are represented by constants S_1 and S_2. The calculation of these constants was developed by Multhopp and is shown in reference [9].

The report of Küchemann and Weber shows that the velocity increase over an infinite sheared wing is given by

$$\left(\frac{V(x,z)}{V_\infty}\right)_{\text{infinite}} = \frac{1+\left(\frac{v_x(x,0)}{V_\infty}\right)_{\Lambda=0}\cos\Lambda}{\sqrt{1+\left(\frac{dz(x)}{dx}\right)^2}} \tag{3.1}$$

In this equation $v_x(x,0)$ represents the velocity component in the direction of the x-axis along the x-axis. The fraction $\frac{dz(x)}{dx}$ represents the curvature of the profile. Λ represents the sweep angle, with aft sweep being positive.

The velocity increase over the root section of a wing is given by

$$\left(\frac{V(x,z)}{V_\infty}\right)_{\text{root}} = \frac{1+\left(\left(\frac{v_x(x,0)}{V_\infty}\right)_{\Lambda=0} - f(\Lambda)\frac{dz(x)}{dx}\right)\cos\Lambda}{\sqrt{1+\left(\frac{dz(x)}{dx}\right)^2}} \tag{3.2}$$

The function $f(\Lambda)$ represents an additional term to the local source strength, which is caused by the root effect. It is given by

$$f(\Lambda) = \frac{1}{\pi} ln \frac{1+\sin\Lambda}{1-\sin\Lambda} \tag{3.3}$$

Equations 3.1 and 3.2 can be simplified by replacing certain expressions with the interference coefficients S_1 and S_2, developed by Multhopp.[9] The simplified results are given by

$$\left(\frac{V(x,z)}{V_\infty}\right)_{\text{infinite}} = \frac{1+S_1\cos\Lambda}{\sqrt{1+{S_2}^2}} \tag{3.4}$$

and

$$\left(\frac{V(x,z)}{V_\infty}\right)_{\text{root}} = \frac{1+\left(S_1 - f(\Lambda)S_2\right)\cos\Lambda}{\sqrt{1+{S_2}^2}} \tag{3.5}$$

Using the Bernoulli equation, the pressure coefficient can be written as:

$$C_\text{p} = 1 - \left(\frac{V}{V_\infty}\right)^2 \tag{3.6}$$

Using Bernoulli's equation the pressure coefficient for both the infinite and finite wing can be found. The pressure coefficient for the infinite sheared wing becomes

$$C_{\text{p ,infinite}} = \frac{-2\cos\Lambda S_1 - {S_1}^2\cos^2\Lambda + {S_2}^2}{1+{S_2}^2} \tag{3.7}$$

while the pressure coefficient of the root section becomes

$$C_{\text{p ,root}} = \frac{-2\cos\Lambda\left(S_1 - f(\Lambda)S_2\right) - \left(S_1 - f(\Lambda)S_2\right)^2\cos^2\Lambda + {S_2}^2}{1+{S_2}^2} \tag{3.8}$$

At this point an important assumption is made. It is assumed that the flow over the outboard part of the wing behaves like the flow over an infinite sheared wing, as was shown in Section 2.3. Therefore, Equations 3.7 and 3.8 represent the pressure coefficients for the outboard and root sections, respectively. Therefore, the difference between the two is the root effect due to thickness, given by:

$$\delta C_{\text{p ,thickness}} = C_{\text{p ,root}} - C_{\text{p ,infinite}} = \frac{\cos\Lambda f(\Lambda)S_2\left(2 - S_2 f(\Lambda)\cos\Lambda + 2S_1\cos\Lambda\right)}{1+{S_2}^2} \tag{3.9}$$

δC_p represents the difference in pressure coefficient between the outboard and root section, in this case due to thickness.

3.1.2 MATRICS-V

In order to show the accuracy of all the results in this report, a method of verification is needed. In Table 3.1 a number of Computational Fluid Dynamics (CDF) methods are compared. The method used for verification should be a method with a higher level of 'fidelity'. All the CDF methods used in development of the root design method are either a Vortex Lattice Method (VLM) or a 2-dimensional panel method. Therefore, the verification method should be a full potential method or higher.

MATRICS-V is a full-potential boundary layer flow solver, developed at the National Aerospace Laboratory (NLR) in the Netherlands. It can calculate the flow over wings and wing-body combinations in subsonic and transonic conditions. The method consists of two parts; an inviscid full potential solver and a viscous boundary layer solver. An interaction algorithm is used to couple the two parts [11].

The first reason for choosing MATRICS-V as a method of verification is that it is a method with a higher 'fidelity' than the methods used for development of the root design method. Table 3.1 clearly shows this, since it uses the full potential equations instead of the linearised ones, it has an 'exact' method for calculating compressibility and it can handle weak shockwaves. The second reason for choosing MATRICS-V is that its validity has been shown by comparing computational results of a Fokker 100 wing/body combination with windtunnel data and flight test data. It was found that the method is in good agreement with these windtunnel results. This validation is shown in reference [12].

All MATRICS-V data was generated using a Mach number of 0.2 and a Reynolds number of 20 000 000. The reason for this is that these values represent low subsonic flying conditions. These conditions produce a

	Vortex Lattice Method	Panel Solver	Full Potential Solver
Governing equations	Linearised potential flow equations	Linearised potential flow equations	Full potential flow equations
Compressibility	Using compressibility corrections	Using compressibility corrections	'Exact'
Lift coefficient	Yes	Yes	Yes
Shockwave prediction	No	No	Inaccurate for strong shocks
Pressure distribution on surface	Maybe (inaccurate at leading edge)	Yes	Yes
Computation time per case	5 sec. - 1 min.	1 min. - 15 min.	5 min. - 1 hr.

Table 3.1: Comparison of CDF methods [10].

minimum of compressive, viscous and shockwave effects. This is desirable because these effects are modelled differently by the different methods, which would produce different results.

Looking at the comparison between the methods, MATRICS-V might even seem like a good candidate to use in the method developed for wing root aerofoil design. The computation times listed in Table 3.1, however, show that for MATRICS-V computations take too long for use in an iterative conceptual design method, as was explained in Section 2.1.

3.1.3 ACCURACY

When implementing the method of Küchemann and Weber in another method, it is important to know the accuracy of this method on its own. This section investigates the accuracy of the method by comparing it with a number of other results.

First of all, the report of Küchemann and Weber shows a comparison for calculations of the velocities over a Royal Aircraft Establishment (RAE)-101 aerofoil with a thickness-chord ratio of 12% [8]. This comparison is shown in Figure 3.1. Overall, the method is in good agreement with the experimental data. However, it can be seen that the root and tip effects are slightly underestimated, as the experimental data shows a larger change with respect to the 'infinite sheared' outboard wing. Another noticeable effect is the lower values of the velocity of the 'infinite sheared' outboard wing around the maximum thickness point. It was found that this error, for the most part, is related to the interpolation of the aerofoil data points. This interpolation influences the Multhopp interference coefficients S_1 and S_2, which in turn influence the results of the method.

The estimation of the root effect due to thickness, is a combination of the equations for the pressure distribution over the surface at the outboard wing and at the wing root, shown in Equations 3.7 and 3.8 respectively. Therefore, when determining the accuracy of the entire method, it is important to know the accuracy of the two parts. Figure 3.2 shows the pressure distribution over an infinite, thirty degree sheared wing with a National Advisory Committee for Aeronautics (NACA)0008 aerofoil, at zero degree angle of attack. For comparison the pressure distribution at half-semi-span of a MATRICS-V run is plotted. For this MATRICS-V run also a NACA0008 aerofoil was used in an untapered, thirty degree sheared wing with an aspect ratio of eight. As can be seen in Figure 3.2, both methods produce similar results. This leads to the conclusion that Equation 3.7 gives a good approximation of the pressure distribution over the outboard section of a wing at zero degree angle of attack with a symmetrical aerofoil.

The pressure distribution over the root section is estimated by Equation 3.8. Figure 3.3 shows the result of such an estimation over a thirty degree sheared wing with a NACA0008 aerofoil. This data is compared to the pressure distribution over the root section of a MATRICS-V run. The same MATRICS-V run is used, of a thirty degree sheared wing with an aspect ratio of eight and a NACA0008 aerofoil. As can be seen in Figure 3.3, the estimation of Equation 3.8 is in good agreement with the MATRICS-V results. Only near the leading edge the pressure estimated is slightly lower than that predicted by MATRICS-V. Küchemann and Weber state that this may be the result of an assumption made for the relation between the free-stream velocity and the velocity along the x-axis.[8] From this it can be concluded that Equation 3.8 gives a good approximation of the pressure distribution over the surface at the root of a wing at zero angle of attack with a symmetric aerofoil.

Since both Equations 3.7 and 3.8 show good agreement with the MATRICS-V results, it can be concluded that Equation 3.9 is a good estimate of the root effect on a wing at zero angle of attack with a symmetric

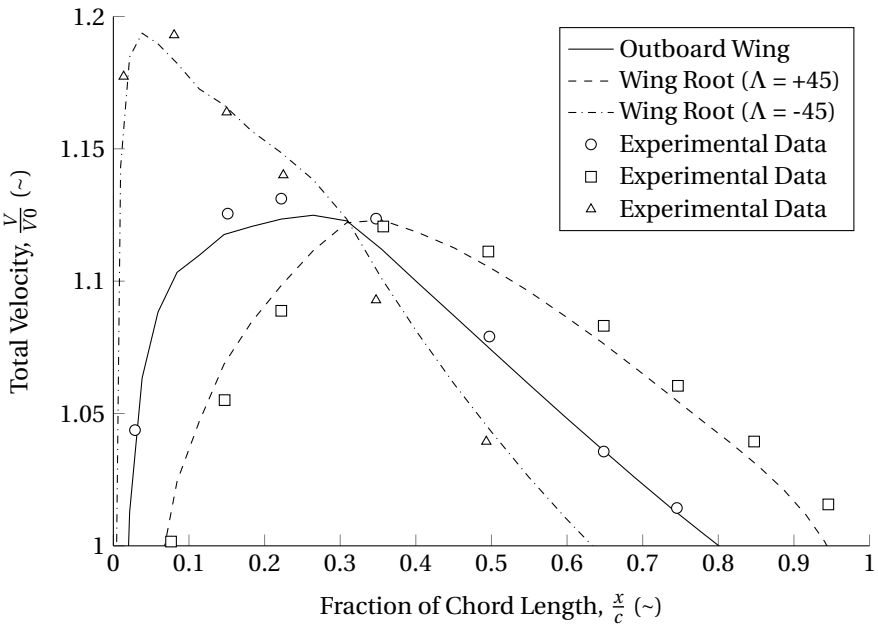

Figure 3.1: Velocity comparison, Küchemann-Weber method vs. experimental data [8].

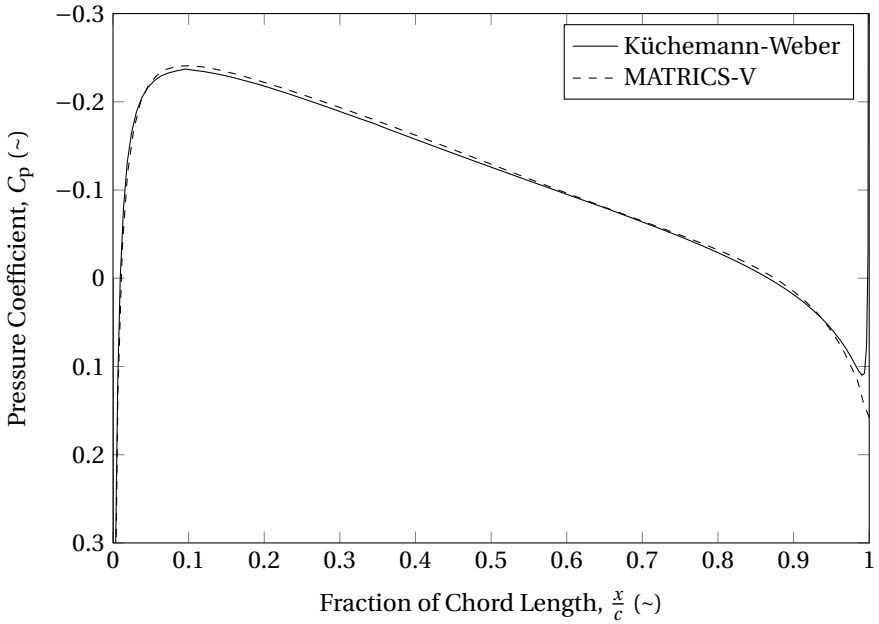

Figure 3.2: Pressure Coefficient comparison for outboard wing.

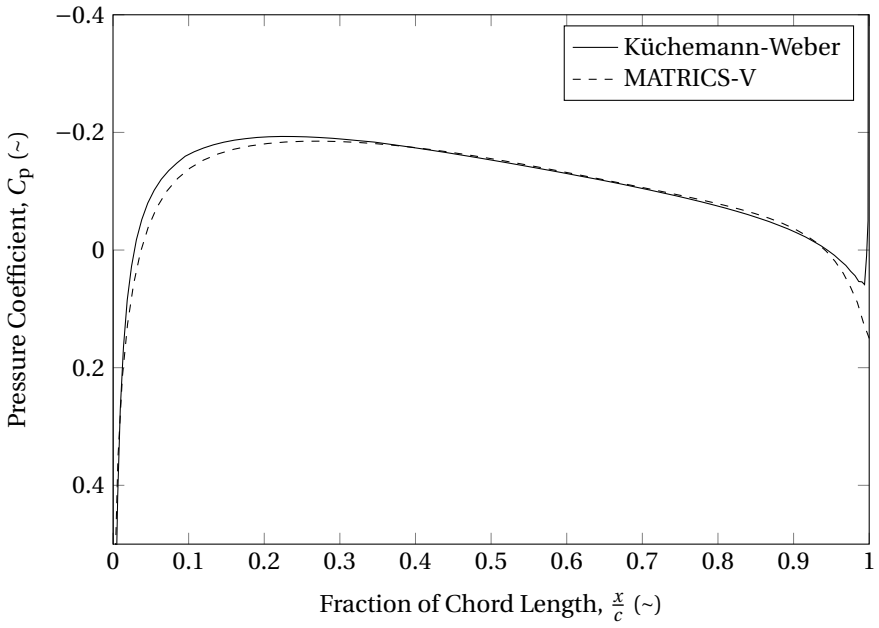

Figure 3.3: Pressure Coefficient comparison for the wing root.

aerofoil. For the pressure distribution on an aerofoil at non-zero angles of attack the reader is referred to Section 3.2.

3.1.4 APPLICATION TO LIFTING SURFACES

The method of Küchemann and Weber is strictly speaking only valid for symmetrical aerofoils at a zero degree angle of attack. It can only calculate the pressure distribution in these conditions. However, in Section 2.3 it was shown that the root and tip effects can be separated into a part caused by lift and a part caused by thickness. In line with this assumption, only the thickness part is considered. Therefore the assumption is made that for the Küchemann-Weber method, the angle of attack and camber of an aerofoil can be ignored. Hereby the aerofoil is reduced to a thickness distribution. In Figure 3.4 is shown how aerofoil camber is removed to estimate the root effect due to thickness.

Since all asymmetrical factors are ignored and therefore removed, it can be assumed that the root effect due to thickness has an equal influence on the upper and lower surface of the aerofoil. Therefore:

$$\delta C_{p\,,\text{thickness,upper}} = \delta C_{p\,,\text{thickness,lower}} = \delta C_{p\,,\text{thickness}} \tag{3.10}$$

Since the separation of the root and tip effects into a thickness and a lift part is purely academic, there

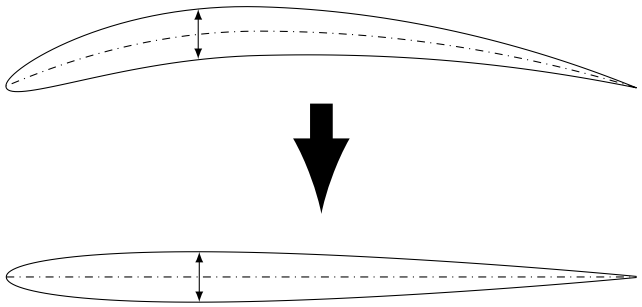

Figure 3.4: Removing Camber from a NACA 9408 aerofoil.

is no data to verify the results of the thickness method on cambered aerofoils. Therefore the verification of ignoring camber for this method will have to be shown using the results of the full method. These results can be found in Section 4.2.

3.2 ROOT EFFECT DUE TO LIFT

As described in Section 2.3 the root effect consists of two parts, a part attributed to thickness and a part attributed to lift. This section describes and verifies the method used to estimate the root effect due to lift. The method is explained in Section 3.2.1. The accuracy and validity of the method are discussed in Section 3.2.2.

3.2.1 LIFT METHOD

The basis for the method described in this section is the report titled "A Simple Method for Calculating the Span and Chordwise Loading on Straight and Swept Wings of any Given Aspect Ratio at Subsonic Speeds", written by Küchemann in 1952 and shown in reference [13]. It is basically a modified lifting surface theory. In this method the wing is represented by a series of horseshoe vortices. This way the wing is modelled as a flat plate, in other words a wing with zero thickness. By solving a series of linear equations, the spanwise lift coefficients can be calculated, along with the spanwise downwash. The chordwise distribution of the pressure differential ΔC_p and aerodynamic centre can also be calculated. For this, use is made of a shape parameter t, which mainly depends on the aspect ratio.

The method has a number of limitations. First, while the method can handle wings of different aspect ratios, it only deals with untapered wings. Secondly, the method models the wing as a flat plate. It does not take the aerofoil shape into account and therefore does not model camber. Despite these limitations, the method is used for tapered wings as well as specific aerofoil shapes, including aerofoil camber. This introduces inaccuracies. The effect of applying the method to non-zero thickness aerofoils is shown in Section 3.2.2. The effect of applying aerofoil camber is shown in Section 3.2.3. For the accuracies of the entire method for determining the pressure distribution over the wing root aerofoil, including wing taper, the reader is referred to Section 4.2.

For estimating the root effect due to lift, the ΔC_p calculation is only necessary for two points along the span. As will be explained in Chapter 4, the section lift coefficients are not calculated using the method by Küchemann, but instead are obtained from a VLM. The reason for this is that a VLM is more versatile, and can handle aerofoil camber and wing taper. Therefore, the Küchemann method is only used for the chordwise estimation of the pressure differential. In this estimation, the root effect is modelled with the k parameter, which is a part of the shape parameter t. This will be shown in the following part.

The first step in estimating the root effect due to lift is to calculate effective sweep angle as defined in the method by Küchemann:

$$\Lambda_{\text{eff}} = \frac{\Lambda_{c/2}}{\left(1 + \left(\frac{a_0 \cos(\Lambda_{c/2})}{A\pi}\right)^2\right)^{1/4}} \tag{3.11}$$

In this equation, $\Lambda_{c/2}$ represents the semi-chord sweep angle. Since all other parts of the method use the quarter chord sweep angle $\Lambda_{c/4}$, this angle has to be calculated using the wing geometry. The lift slope coefficient of the two-dimensional aerofoil is given by a_0 and A represents the wing aspect ratio.

The next step in determining the root effect due to lift is to calculate the interpolation function for the shift in aerodynamic centre k. This forms the basis of the root and tip effect due to lift. The interpolation function k is dependent on the y co-ordinate in terms of the chord length, y_c. Since the Küchemann method is assuming that the wing is not tapered, y_c can be rewritten to:

$$y_c = \frac{1}{2} y_{\text{pos}} A \tag{3.12}$$

where y_{pos} is the spanwise fraction from root to tip. For determining the root effect due to lift, an interpolation function k is introduced. The k function for the root section can be written as:

$$k(y_c)_{\text{root}} = \sqrt{1 + (2\pi y_c)^2} - 2\pi y_c \tag{3.13}$$

At the wing tip the function is mirrored and the inverse of the root function:

Figure 3.5: Spanwise distribution of the interpolation function k for a wing with an aspect ratio of 8.

$$k(y_c)_{tip} = -\sqrt{1 + \left(2\pi\left(A/2 - y_c\right)\right)^2} - 2\pi\left(A/2 - y_c\right) \tag{3.14}$$

The total interpolation function, k, is given by:

$$k(y_c) = k(y_c)_{root} + k(y_c)_{tip} \tag{3.15}$$

An example of the spanwise k distribution is shown in Figure 3.5, for a wing with an aspect ratio of 8.

With k known, the shape parameter t can be calculated. It is given by:

$$t = 1 - \frac{1 + k(y_c)\frac{\Lambda}{\pi/2}}{2\left(1 + \left(\frac{a_0 \cos\Lambda}{\pi A}\right)^2\right)^{\frac{1}{4\left(1+|\Lambda|\frac{1}{2}\pi\right)}}} \tag{3.16}$$

The shape parameter t forms the basis of the calculation of the chordwise pressure differenctial, ΔC_p. ΔC_p is the difference between the pressure coefficient C_p of the lower and the upper surface of the wing. The chordwise pressure differential therefore represents the lift generated along the chord. It is calculated using:

$$\Delta C_p(x) = -\frac{\sin \pi t}{\pi t} c_l \left(\frac{1-x}{x}\right)^t \tag{3.17}$$

in which c_l represents the sectional lift coefficients. The are obtained from the spanwise lift estimation made by Athena Vortex Lattice (AVL), as is shown in Chapter 4.

As stated earlier, the calculation to find the chordwise pressure differential ΔC_p is performed at two separate positions along the span. The purpose of this is to be able to find the root effect. It is assumed that the outboard (or half semi-span) part of the wing is barely influenced by the interpolation function k and therefore the root effect. Looking at the k distribution shown in Figure 3.5, which forms the basis for the root effect, it can be seen that this is a reasonable assumption. Therefore, when subtracting the outboard 'undisturbed' chordwise pressure differential ΔC_p from the root ΔC_p, only the root effect due to lift remains.

The resulting difference in chordwise pressure differential ΔC_p represents the root effect due to lift. It is still defined in terms of pressure differential ΔC_p, the difference between the upper and lower surface pressure coefficients. However, for the final result, the actual upper and lower surface pressure coefficients δC_p are needed. Some method has to be found to divide the pressure differential ΔC_p into a part that can be attributed to the upper surface and a part that can be attributed to the lower surface. As an initial estimate, the parts for upper and lower parts are assumed to be equal. Chapter 4 will treat this division in more detail.

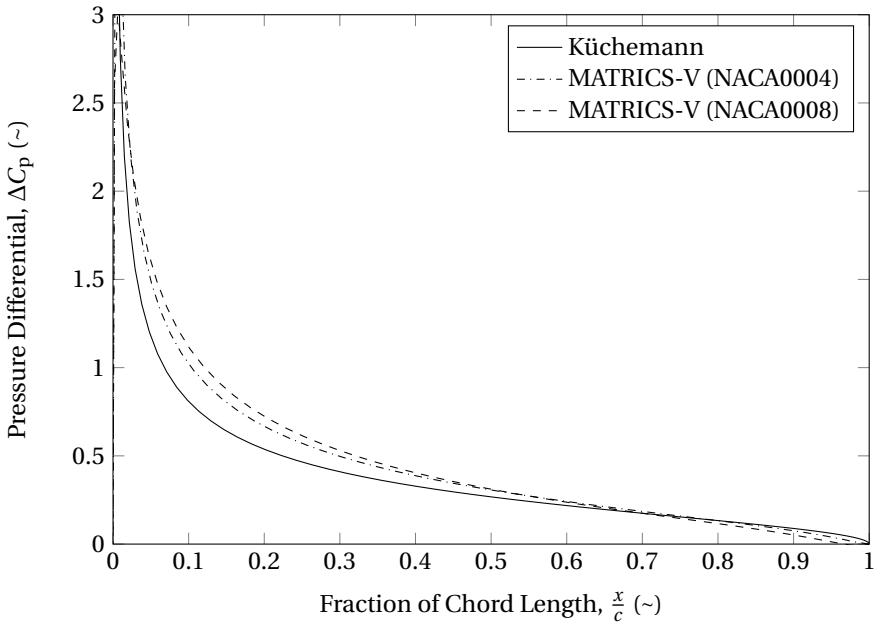

Figure 3.6: Chordwise pressure differential on the outboard section of a 30 degree swept back untapered wing with an aspect ratio of 8, at a 6 degree angle of attack.

3.2.2 ACCURACY

When using the Küchemann method as part of a method to predict the root pressure distribution, it is important to understand the accuracy of the method on it's own. This section compares the pressure differentials of an outboard section and a root section to MATRICS-V data for the same cases. Also the resulting root effect due to lift is compared to MATRICS-V data. Since the method only produces a pressure differential, and not a pressure distribution, it has to be compared to the pressure differential from the MATRICS-V data.

Using MATRICS-V data to show the accuracy of the root effect due to lift is difficult, since it is not possible to separate the lift and thickness part in the data. In the case of the root effect due to thickness, lift can be eliminated, since a symmetrical aerofoil at a zero degree angle of attack has a sectional lift coefficient of zero. Thickness however, can not be eliminated because MATRICS-V does not allow computation for surface with no thickness. It would be possible to reduce the effect of thickness by using the Küchemann-Weber method for thickness, shown in Section 3.1. This however, would cloud the data by introducing inaccuracies from this method, which would impair the ability to look at the accuracy of the Küchemann method for lift alone.

Figure 3.6 shows the pressure differential, the difference between the upper and lower pressure surface pressure coefficient, for the outboard section of a swept wing at an angle of attack. It can be seen that, overall, the results of the Küchemann method are in good agreement with the MATRICS-V data. The pressure differential is underestimated near the maximum thickness point and slightly overestimated near the trailing edge. Also, it can be seen that with decreasing thickness, from NACA0008 to NACA0004, the results become more accurate. This is in agreement with theory, since the Küchemann method is essentially a flat plate approximation. Therefore it can be assumed that a large part of the difference shown in Figure 3.6 is caused by thickness. In the total method this should be corrected by the model for the thickness part shown in Section 3.1.

The pressure differential for the root section of a swept wing at an angle of attack is shown in Figure 3.7. The accuracy is similar to that of the outboard section. The results are in good agreement. Again an underestimation near the point of maximum thickness and a slight overestimation near the trailing edge is observed. Once again the results become more accurate with decreasing thickness, as can be expected with the flat plate approximation used by Küchemann. Therefore a large part of the difference can be attributed to the effect of thickness, which will be corrected by the thickness estimation in the complete method.

Figure 3.8 shows the final result of the Küchemann method in predicting the root effect due to lift. It is the difference in pressure coefficient from an outboard section to a root section, for the upper surface. As was explained in Section 3.2.1, the pressure differential of the outboard section is subtracted from that of the root section, leaving the root effect. This is then split into two equal parts for the upper and lower surface.

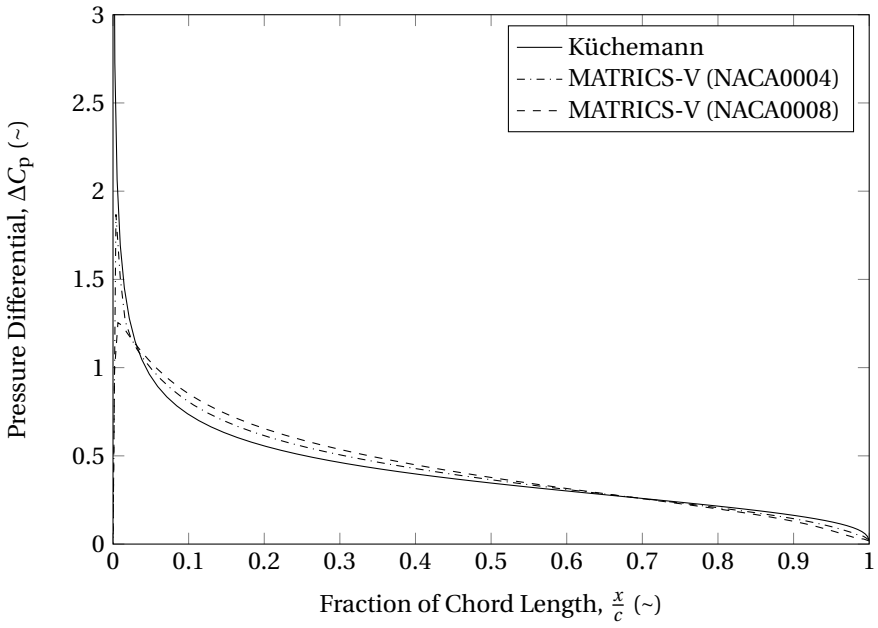

Figure 3.7: Chordwise pressure differential on the root section of a 30 degree swept back untapered wing with an aspect ratio of 8, at a 6 degree angle of attack.

In Figure 3.8 these values are compared with the change in upper surface pressure coefficient between the outboard and the root section of the MATRICS-V data.

Similar to the pressure differential shown in Figures 3.6 and 3.7, it shows an underestimation near the maximum thickness part and a slight overestimation near the trailing edge. Generally however, it is in good agreement with the MATRICS-V data. It can be seen that with decreasing thickness, the differences become smaller. This is to be expected since the Küchemann method uses a flat plate approximation. However, another effect plays a role here. It was assumed that the lift effect is equally divided between the upper and lower surface. Therefore, the difference in pressure differential is split into two equal parts. This however, is probably not the case. The lift effect might have more effect on the upper surface than on the lower surface. This would change the Küchemann results shown in Figure 3.8, and therefore the accuracy. At the moment however, there is no method for a chordwise distribution of the root effect due to lift between the upper and lower surface. Therefore a simple division into equal parts is used.

3.2.3 APPLICATION TO CAMBERED SURFACES

The method to estimate the root effect due to lift, taken from Küchemann, is only valid for uncambered aerofoils. However, since it is only dependent on wing planform parameters and the section lift coefficient, it is possible to apply the method to cambered aerofoils. In Figure 3.9 the upper surface pressure difference from outboard to root is compared to the Küchemann method. The sectional lift coefficient for the Küchemann method is calculated using AVL. Looking at Figure 3.9, it can be seen that the results are not in good agreement. There is a large overestimation in the front half of the profile, while the rear half shows an underestimation of the change in pressure coefficient. Part of this can be explained by the thickness. The NACA3408 aerofoil has a thickness similar to the NACA0008 aerofoil, which is shown in Figure 3.8. Especially in the rear half of the profile, the change in pressure distribution shows similarities to that of the NACA0008 aerofoil. In the front half however, the difference can not be attributed to the effect of thickness. Therefore, the results of the root effect due to lift on cambered aerofoils will be less accurate near the leading edge. The resulting effect on the complete method for estimation of the wing root pressure distribution can be seen in Chapter 4.

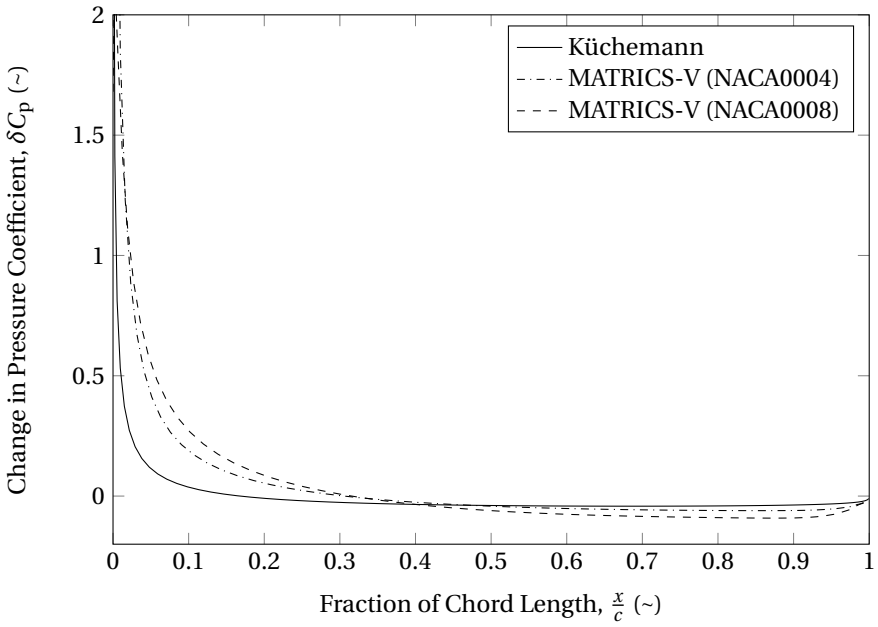

Figure 3.8: Chordwise change in pressure coefficient on the upper surface of a 30 degree swept back untapered wing with an aspect ratio of 8, at a 6 degree angle of attack.

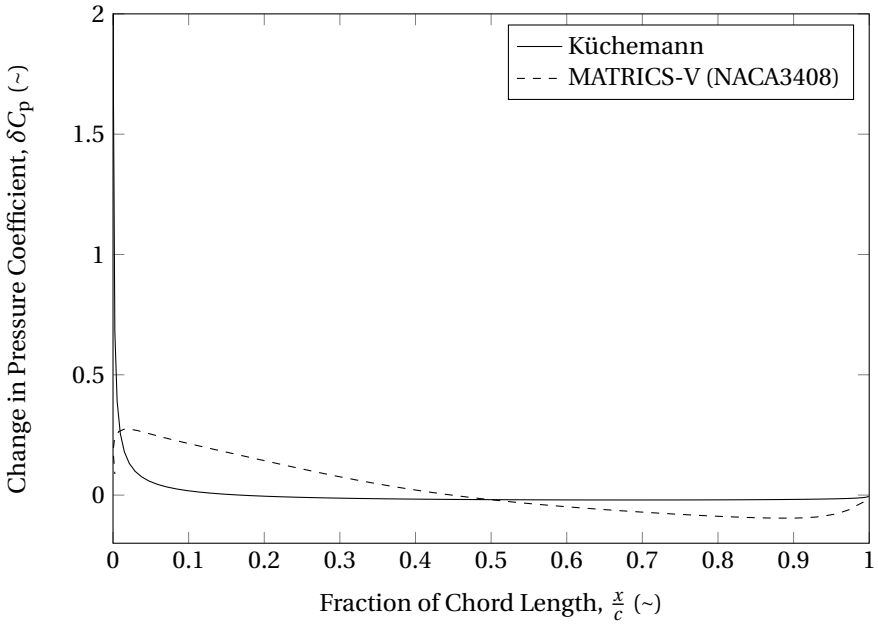

Figure 3.9: Chordwise change in pressure coefficient on the upper surface of a 30 degree swept back untapered wing with an aspect ratio of 8, at a 0 degree angle of attack.

4

Estimation of Root Pressure Distribution

In Sections 3.1 and 3.2 two methods are shown to estimate the root effect due to thickness and lift respectively. In Section 2.3 the assumption is made that the root effect can be separated into a part attributed to thickness and a part to lift. Based on this assumption, the aforementioned methods can be combined to give an estimate of the total root effect. By coupling the methods with a VLM and a two-dimensional panel method, a method is devised to calculate the pressure distribution over the root section of a wing of any regular shape. In Section 4.1, the method for estimating the root pressure distribution is explained. Section 4.2 shows the results of this method and evaluates its accuracy.

4.1 Method

The basic workings of the method for determining the pressure distribution over the root section of a wing are shown in Figure 4.1. The first step is to calculate the spanwise distribution of the lift coefficients. This is done using a VLM called AVL, which will be described in Section 4.1.3. To be able to calculate the spanwise lift, the wing geometric properties will have to be defined using the planform data and the aerofoil. These inputs will be explained in Sections 4.1.1 and 4.1.2.

With the spanwise lift known, the chordwise root pressure distribution can be estimated. The first part to be estimated is the root effect due to thickness. Since this is method only depends on the sweep angle and the root profile, it does not require the results from the spanwise lift. The *Thickness Effect* module will be described in Section 4.1.4. Second part of the root pressure estimation is the root effect due to lift. The *Root Effect* module is dependent on the sectional lift coefficient, but also produces an amount of lift due to the resulting pressure differential, ΔC_p. The thickness part does not produce lift since its effect is assumed to be equal for both upper and lower surface. Since the three modules (*Thickness Effect*, *Lift Effect* and *2D Panel Method*) will be combined to determine the root pressure distribution, their combined lift coefficient will have to match the sectional lift coefficient. Therefore, the lift effect lift coefficient has to be subtracted from the sectional lift coefficient in order obtain the lift coefficient for the panel method. The *Lift Effect* module will be described in Section 4.1.5. The *2D Panel Method*, described in Section 4.1.6, uses the remaining part of the sectional lift coefficient and the aerofoil. The lift coefficient is prescribed to the panel method, which will rotate the aerofoil until the right lift coefficient is found. This way, the panel method finds its own effective angle of attack, which will be lower than the total wing angle of attack due to downwash.

The final step is to add the results from the three modules, to find the chordwise root pressure distribution, which is described in Section 4.1.7.

4.1.1 Planform Data

One of the two inputs for the method is the planform data. Figure 4.2 shows the planform definitions used in this report. The planform data contains all geometrical data of the wing; sweep angle Λ, aspect ratio A, wing span b, taper ratio λ and the kink position y_{kink}. From these inputs, all other geometric data for the wing can be calculated, such as reference area and chord lengths.

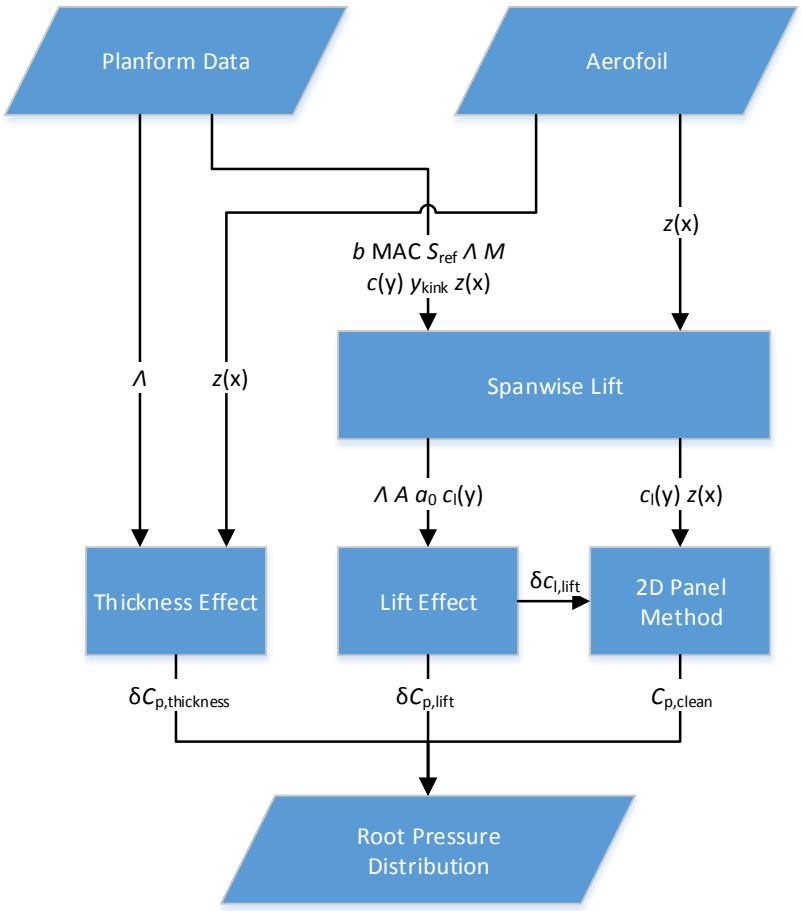

Figure 4.1: Schematic of the method for determining the root section pressure distribution.

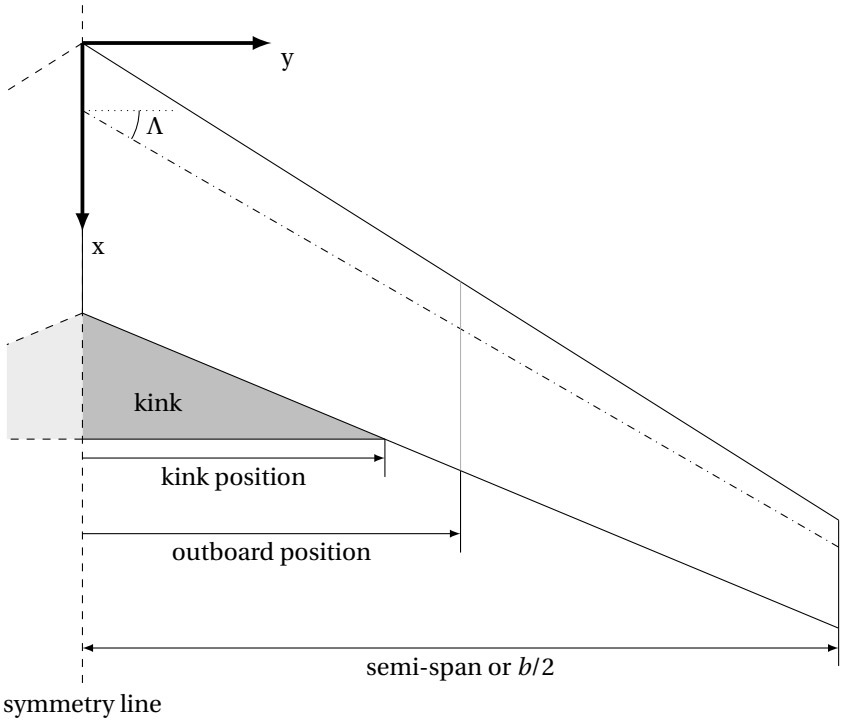

Figure 4.2: Planform definitions.

4.1.2 AEROFOIL

The second part of the inputs for the method is the aerofoil. The aerofoil data can be imported into the method by supplying a *.dat* file. The *.dat* file must have two continuous columns of data, the first column for the x co-ordinates and the second column for the corresponding z co-ordinates. The data can be read in any order; front to back or back to front and upper to lower or lower to upper. The aerofoil data is interpolated onto a cosine distribution along the x-axis. By using a cosine distribution, the density of data points increases towards the leading and trailing edge. An example of a cosine distribution is shown in Figure 4.3. Using a cosine distribution places more emphasis on the leading and trailing edge parts, which usually also have the highest curvature. The cosine distribution is needed for the Küchemann-Weber method for determining the root effect due to lift. This cosine distribution is used throughout the entire method. The first reason for this is the simplicity of not having to work with two different co-ordinate distributions. The second reason is to reduce the number of data interpolations used in the method. Every interpolation reduces the accuracy of the results and therefore should be avoided as much as possible.

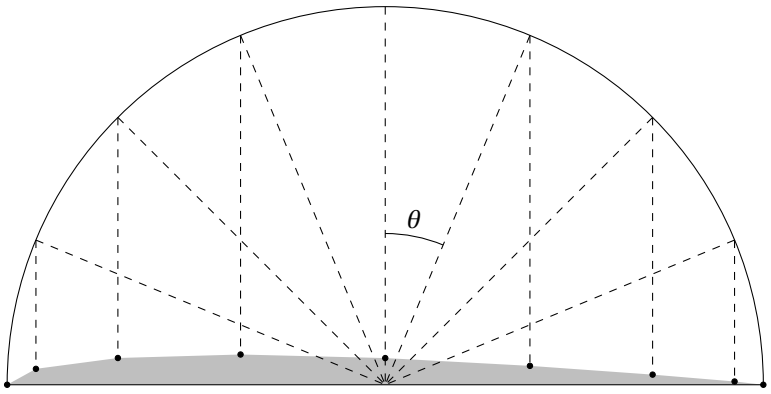

Figure 4.3: Example of a cosine distribution on a NACA0008 aerofoil.

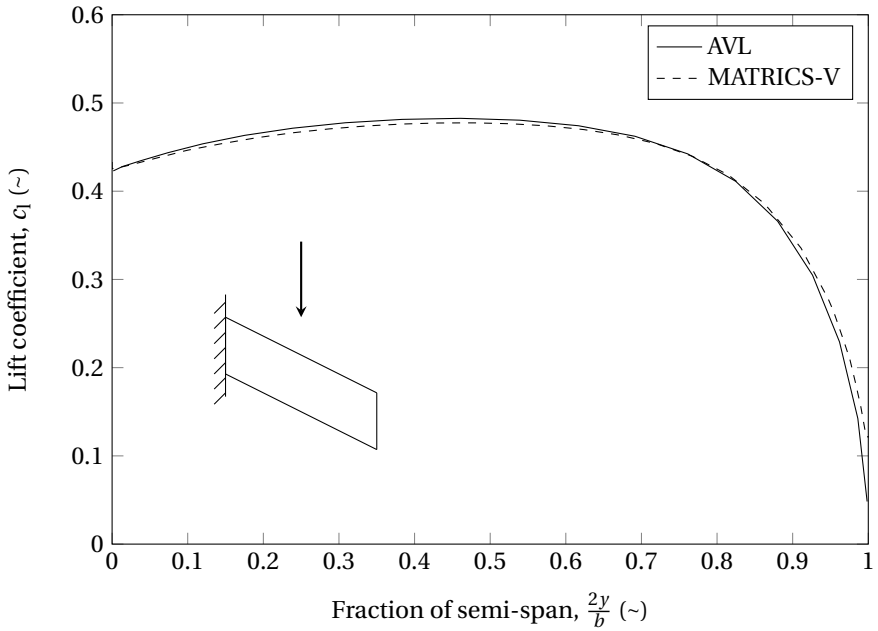

Figure 4.4: Spanwise distribution of the sectional lift coefficient c_l for a 30 degree aft swept wing at a 6 degree angle of attack.

4.1.3 SPANWISE LIFT

The main function of the *Spanwise Lift* module of the method is to estimate the spanwise lift distribution of the wing. As can be seen in Figure 4.1, it uses inputs from the *Planform Data* and *Aerofoil* modules, and supplies the *Lift Effect* and *2 DPanel Method* functions with the spanwise lift distribution. As stated earlier, for estimation of the spanwise lift coefficients, the AVL software is used, which is descibed below.

The *Spanwise Lift* module starts with preparing the input files for a run of the AVL software. The first step is to create the geometry file. To this end it calculates the leading edge positions of the two aerofoil sections, or three if a kink is present. At all two (or three) positions it then adds the chord lengths and finally the aerofoil. The second step is to create the input file. This file contains the commands followed by the software, like loading the geometry file, setting the incidence angle and Mach number and finally writing the output. After running the AVL software with the inputs, it produces output files. From these files, the spanwise lift coefficients are taken.

AVL

AVL is a vortex lattice code intended for rapid aeroplane configuration analysis. It was developed from 1988 onwards by Mark Drela and Harold Youngren at the Massachusetts Institute of Technology. Surfaces in AVL are represented as single-layer vortex sheets, discretised into horseshoe vortex filaments. It is best suited for thin lifting surfaces at small angles of attack and side-slip. AVL becomes less accurate above a Mach number of 0.6.

AVL uses an input file in which the geometry of the configuration is specified. It can handle lifting surfaces with or without specified aerofoil sections and control surfaces. However, it cannot model thickness and therefore uses a 'flat plate' approach. It also has a module for slender bodies. However this should be used with caution because there is little experience with it.

The AVL output file gives the spanwise lift distribution, spanwise lift coefficients, the spanwise induced drag, the total wing lift coefficient, total wing induced drag and moment coefficient. It also gives the position of the aerodynamic centre, albeit not accurate, and the chordwise pressure difference at each station [14].

In the method developed for root aerofoil design, AVL is only used for estimating the section lift coefficients. In order to evaluate the accuracy of the section lift coefficients produced by AVL, they are compared to MATRICS-V data. Figures 4.4 and 4.5 show these comparisons for an aft and a forward swept wing respectively.

Figure 4.4 shows the sectional lift coefficients for an untapered 30 degree aft swept wing at a 6 degree angle of attack. By comparing the AVL and MATRICS-V data, it can be seen that both methods are in good agreement. AVL shows a slight overestimation in the outboard section and a slight underestimation near the

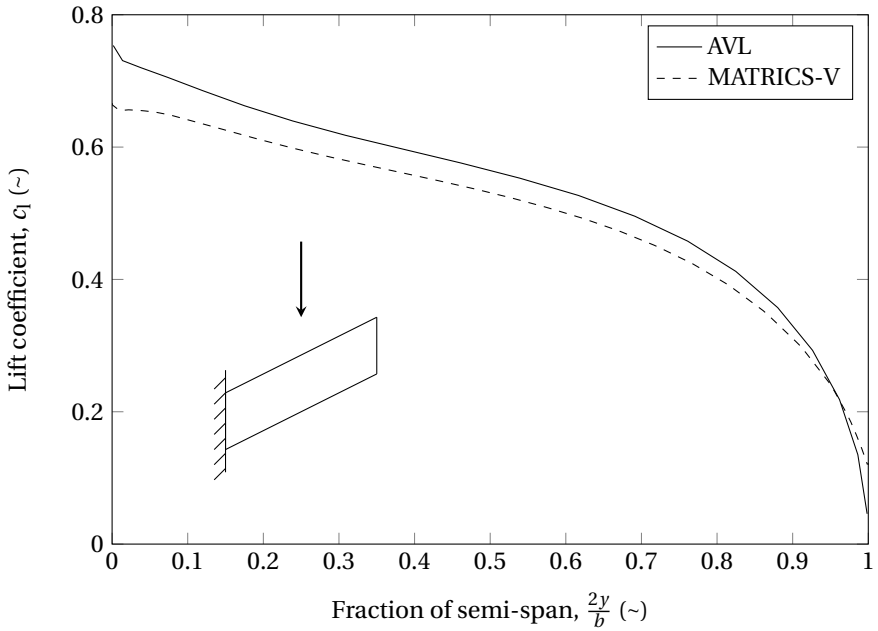

Figure 4.5: Spanwise distribution of the sectional lift coefficient c_l for a 30 degree forward swept wing at a 7.36 degree angle of attack.

tip. Figure 4.5 shows the same wing swept 30 degrees forward. It can be seen that AVL and MATRICS-V have the same general shape, but AVL shows a small underestimation near the wing root.

The differences between the results of both methods are likely caused by the fundamental differences between the two methods themselves. As was shown in Table 3.1, a VLM uses linearised potential flow equations while MATRICS-V uses the full potential flow equations. Because the method developed for root aerofoil design is a conceptual method which requires low computational times, the accuracy of AVL is found to be satisfactory.

4.1.4 THICKNESS EFFECT

The *Thickness Effect* module, as shown in Figure 4.1, estimates the root effect due to thickness according to the method laid out in Section 3.1. This method is only dependent on the aerofoil and the wing sweep angle, Λ. This calculation results in the difference in pressure coefficient, C_p, both for the upper and lower surface of the wing root section. These results are added to the results of the *Lift Effect* and *2D Panel Method* modules and together form the final *Root Pressure Distribution.*

4.1.5 LIFT EFFECT

The *Lift Effect* module estimates the root effect due to lift by using the method shown in Section 3.1. Figure 4.1 demonstrates that it uses the spanwise lift distribution estimated in the *Spanwise Lift* module. It also uses the geometrical wing properties from the *Planform Data.* Because the method uses the semi chord sweep angle $\Lambda_{c/2}$, this angle has to be calculated from the geometrical properties of the wing and the quarter chord sweep angle, Λ. The module however does not use the aerofoil, since the Küchemann method for the lift effect is based on a flat plate approach. The chordwise pressure differential ΔC_p calculated by the *Lift Effect* module is divided between the upper and lower surface of the section. The resulting change in upper and lower surface pressure distribution δC_p is added to the *Thickness Effect* and *2D Panel Method* modules to form the final *Root Pressure Distribution.*

The root effect due to thickness, as explained in Section 3.1, is of a symmetrical nature. Its effect on the upper surface is the same as its effect on the lower surface. The root effect due to lift, explained in Section 3.2 however, is not symmetrical in this regard. The pressure differential ΔC_p decreases the pressure coefficient on the upper surface and increases the pressure coefficient on the lower surface. This difference between upper and lower pressure distribution will result in a contribution to the section lift coefficient δc_l. The magnitude of this δc_l caused by the root effect due to lift can be estimated by making a numerical integration of the ΔC_p for a section with a chord length of one. The resulting contribution to the sectional lift coefficient is passed

on to the *2D Panel Method* module, where it is subtracted from the sectional lift coefficient to be achieved by the panel method.

4.1.6 2D PANEL METHOD

The purpose of the *2D Panel Method* module is to compute the pressure distribution over the 'clean' aerofoil. With 'clean' it is meant that the aerofoil is assumed not to be in any three-dimensional effects such as the root effect. As can be seen in Figure 4.1, the *2D Panel Method* module receives input from the *Spanwise Lift* and *Lift Effect* module. From the *Spanwise Lift* it is supplied with the local sectional lift coefficient, while it uses the same aerofoil and angle of attack. From the *Lift Effect* module the contribution of the root effect due to lift to the sectional lift coefficient is obtained. This is subtracted from the total sectional lift coefficient in order to find the corrected sectional lift coefficient to be used by the panel method. For calculation the *2D Panel Method* uses the Xfoil software, which will be explained below. The panel method is executed in the direction of the free-stream flow.

As shown in Figure 4.1 the resulting pressure distribution is added to the pressure difference due to the thickness and lift effects, leaving an estimation of the full pressure distribution on the root aerofoil.

XFOIL

Xfoil is a two-dimensional inviscid linear-vorticity panel method with Karman-Tsien compressibility correction. It was developed by Mark Drela at the Massachusetts Institute of Technology, to allow for rapid calculation on low Reynolds number aerofoils flows. By using a viscid-inviscid method, the viscous layer influence can be calculated. Because it has these capabilities, it can model flow instability, flow separation, bubble losses, etc. This allows the designer to quickly identify these issues and try new designs approaches. A paper by Mark Drela, shown in reference [15], explains the theoretical basis of Xfoil. It also shows validation of the method by comparing calculations with experimental data.

Because of its low computational times, combined with its validated performance, Xfoil is chosen for use with the root aerofoil design method.

4.1.7 ROOT PRESSURE DISTRIBUTION

The final result of the method is given by the *Root Pressure Distribution* module. As shown in Figure 4.1, it combines the results of the *Thickness Effect*, *Lift Effect* and *2D Panel Method* modules. As explained in their respective modules, the results of the *Thickness Effect* and *Lift Effect* are prepared in such a way that they can simply be added to the results of the *2D Panel Method*. The final result is the estimated pressure distribution over the root aerofoil of a specified wing, including the root effect.

4.2 RESULTS

In the previous section, 4.1, a method is developed to estimate the pressure distribution over the root section of a wing of given shape with a given aerofoil. This method is based on two other methods, shown in Sections 3.1 and 3.2. Even though the accuracy of both methods was shown, it is important to evaluate the accuracy of the complete method. This will show the result of combining the methods with the spanwise lift estimation and the panel method.

Section 4.2.1 will focus on the most simple case of an untapered wing with symmetrical aerofoils. The results of using a cambered aerofoil are shown in Section 4.2.2. Section 4.2.4 will show the effect of taper while Section 4.2.5 will show the results for a wing with a kink.

4.2.1 SYMMETRIC AEROFOILS

As a first estimate of the accuracy of the method, the results for a 30 degree swept back, untapered wing with a symmetrical NACA0008 aerofoil is shown in Figure 4.6. The root pressure distribution is calculated by the method explained in Section 4.1, and compared with results from a MATRICS-V analysis.

The pressure distribution at the top of Figure 4.6 shows the aforementioned wing at a 0 degree angle of attack. Since there is no lift, the results should correspond to the results of the method for estimating root effect due to thickness. A comparison with Figure 3.3 shows that this is indeed the case. In both cases the method and MATRICS-V results are in good agreement, with only a small overprediction near the leading edge.

The results shown in Figure 3.3 are for the method for root effect due to lift only. For the results of the method, shown in Figure 4.6, the root effect due to thickness is isolated and superimposed on the results of

the panel method, as explained in Section 4.1. The fact that both results are in good agreement shows that using the panel method produces accurate results.

The middle and lower data shown in Figure 4.6 correspond to increasing angles of attack; 3 and 6 degrees respectively. As can be seen, both methods are in good agreement for most of the positions. However, near the leading edge an overprediction shows, mostly on the upper surface, which is increasing with increasing angle of attack. This effect is most likely caused by the estimation of the root effect due to lift, which also shows an overestimation near the leading edge, as shown in Figure 3.8.

4.2.2 CAMBERED AEROFOILS

The second part in determining the accuracy of the method is the addition of aerofoil camber. The results for a 30 degree swept back, untapered wing at a 0 degree angle of attack are shown in Figure 4.7. At the top, a NACA0008 aerofoil is shown. Moving down, the camber of the aerofoil is increased, resulting in a NACA3408, NACA6408 and a NACA9408 aerofoil.

Since there is positive camber and a 0 degree angle of attack, for most of the chord length, the upper and lower surface pressure distribution 'switch'. The lower surface pressure distribution is shown above the upper surface pressure distribution.

As camber is increased, the pressure distribution is in good agreement for all chordwise position downstream from the 0.5 fraction of chord length. Upstream from this position, 0.0 to 0.5 fraction of chord length, the method underestimates the upper surface pressure and overestimates the lower surface pressure. This inaccuracy is most likely caused by the fact that the method for estimating the root effect due to lift is not valid for cambered aerofoils. This is investigated in Section 3.2.3. Figure 3.9, which shows this inaccuracy, shows a similar underestimation on the upper surface.

4.2.3 FORWARD SWEEP

All the chordwise pressure distributions shown so far, have been for aft swept wings. Since the method should also be applicable to forward swept wings, it is important to evaluate the performance for this case. In Figure 4.8 a comparison is given of MATRICS-V data and the Method for a 30 degree forward swept wing with a NACA0012 aerofoil at a 7.36 degree angle of attack.

From Figure 4.8 it can be seen that the method is less accurate for the forward swept case. The pressure differential ΔC_p of the method, the difference between the upper and lower surface pressure coefficient, has a higher value for almost all chordwise positions. This means there is a difference in section lift coefficient c_l. The cause for this difference is likely due to the inaccuracy in the sectional lift coefficient as estimated by AVL. This difference in sectional lift coefficient can be seen in Figure 4.5, for which the same data set is used. The general trend, however, shows good agreement.

4.2.4 EFFECT OF TAPER

The second geometrical aspect to be investigated is the wing taper ratio. In Figure 4.9 the effect of changing wing taper on the method is shown. As is indicated in the figure, the top line for both methods has a taper ratio of 1.0. Going down the second line has a taper ratio of 0.6 and the lowest line has a taper ratio of 0.2. In order to have data from similar cases as much as possible, the aspect ratio is kept the same. For different values for the wing taper ratio, this means changing the wing chordlengths. This was chosen since the method does not respond to changes chordlength, but does react to changes in aspect ratio. In Figure 4.9 a comparison is shown for the root pressure distribution between MATRICS-V results and results of the method on an aft swept wing with a NACA0008 aerofoil.

From the method, it is known that the taper ratio only has an effect on the spanwise analysis of the lift coefficients, by AVL. Different taper ratios result in different section lift coefficients at the root, resulting in a different pressure distribution. From Figure 4.9 can be seen that both methods show a similar response to the change in taper ratio. The difference between the results stays the same as for the untapered case, also shown in Figure 4.6. Taking this into account, it can be concluded that for a change in taper ratio, both methods are in good agreement.

4.2.5 EFFECT OF WING KINK

The final wing geometry parameter to be evaluated is the presence of a wing kink. The method itself has no way of taking a wing kink into account, other than its effect on the aspect ratio. Since for the method, the aspect ratio is fixed, the surface area of the kink is taken into account when calculating the different chord

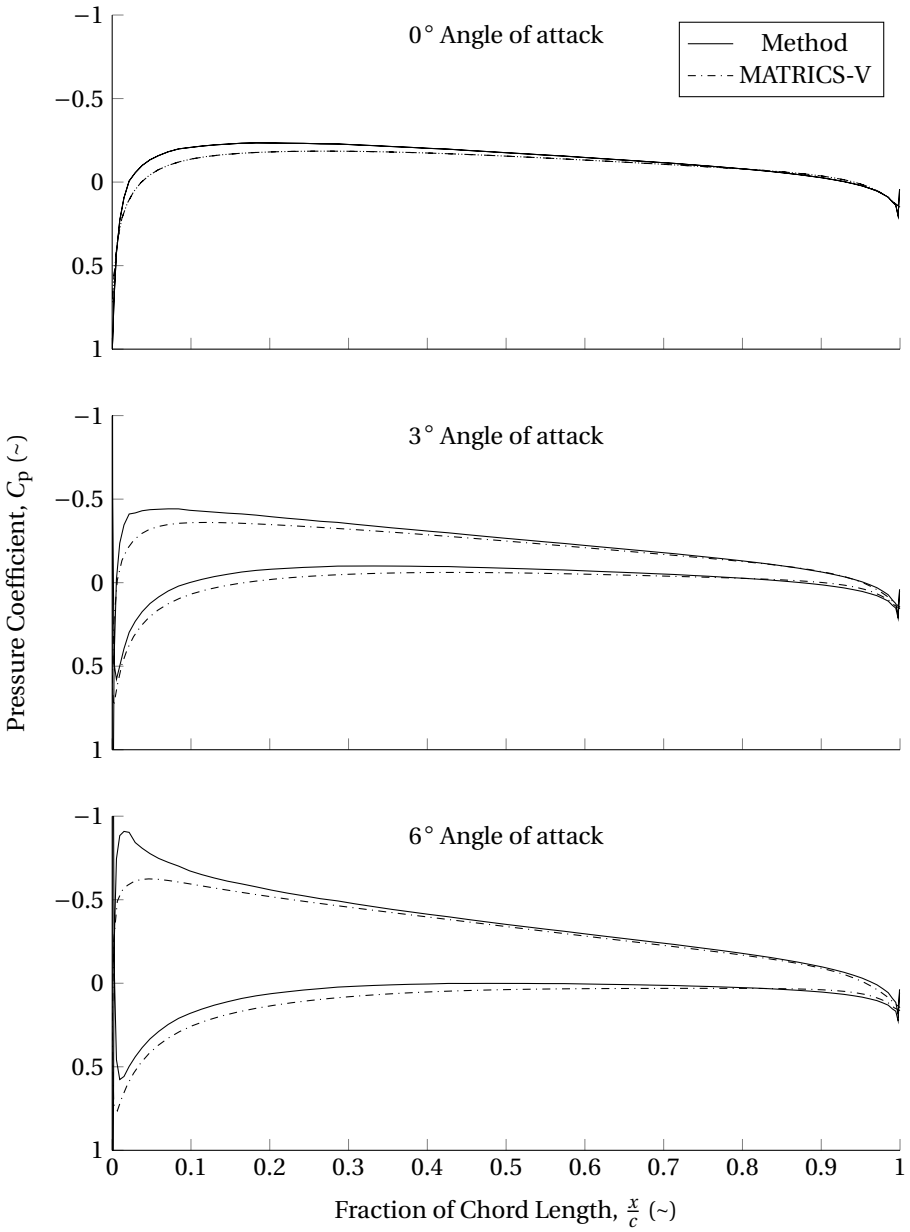

Figure 4.6: Root pressure distribution of a wing with a NACA0008 aerofoil at a different angles of attack.

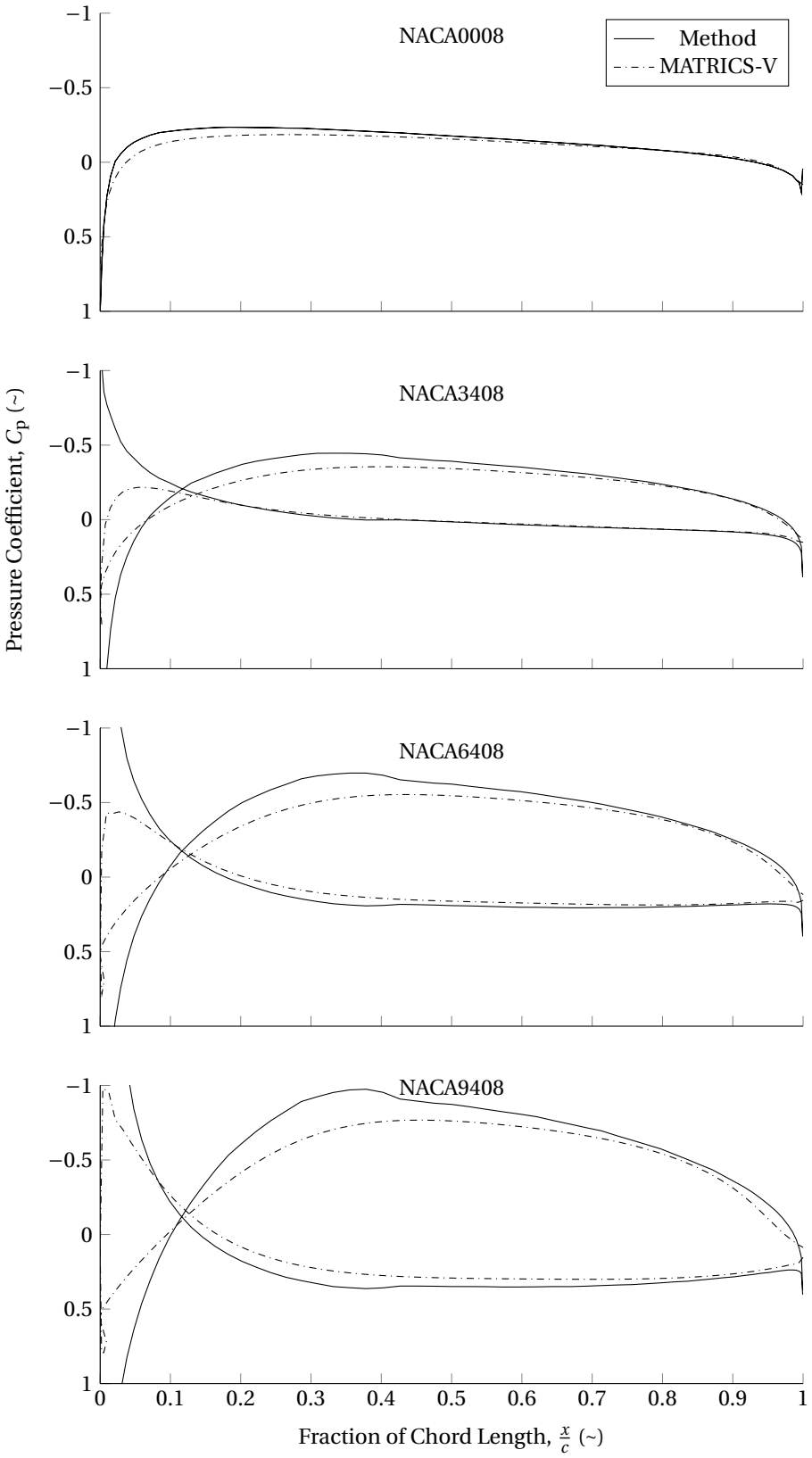

Figure 4.7: Root pressure distribution of a wing with different cambered aerofoils at a 0 degree angle of attack.

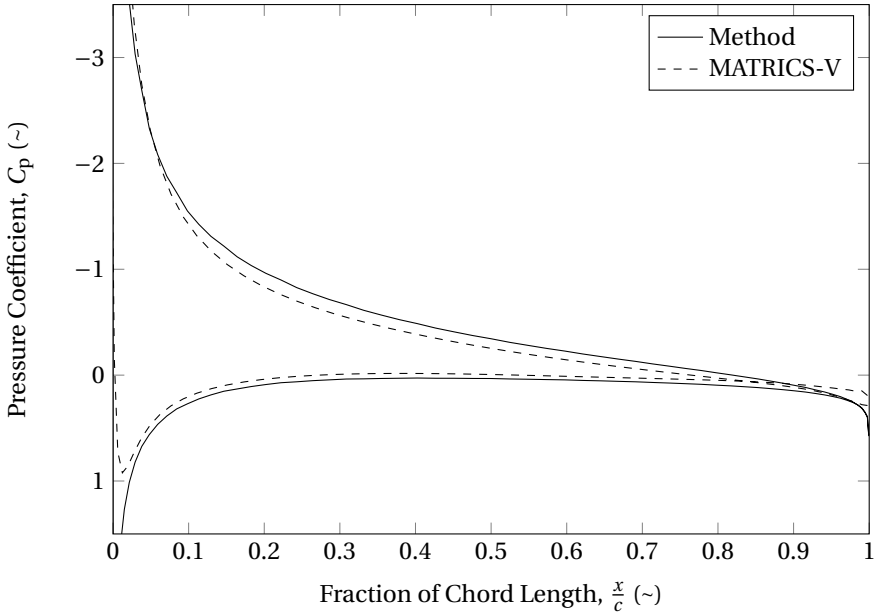

Figure 4.8: Root pressure coefficient comparison for an untapered forward swept wing with a NACA0012 aerofoil at a 7.36 degree angle of attack.

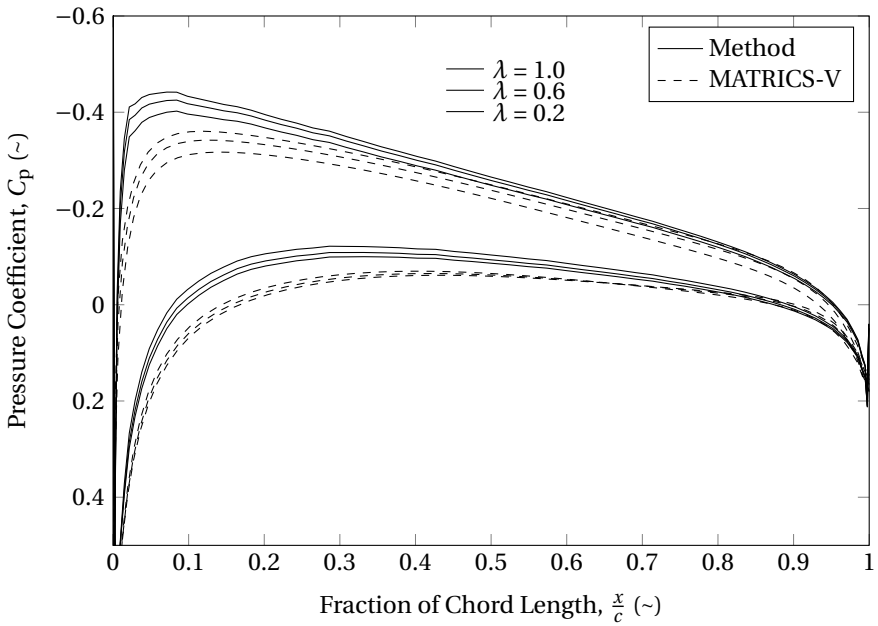

Figure 4.9: Pressure coefficient comparison for different taper ratios on a wing with a NACA0008 aerofoil at a 3 degree angle of attack.

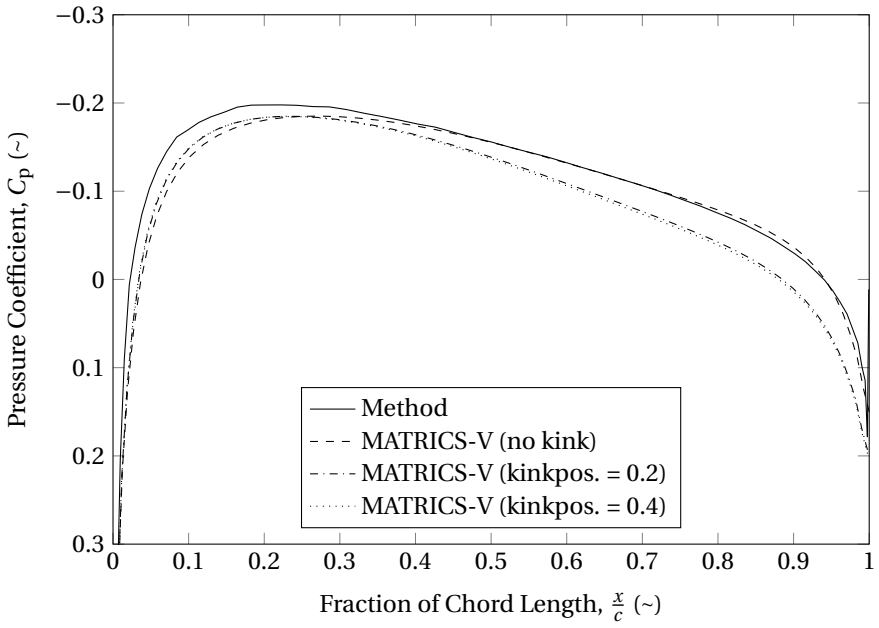

Figure 4.10: Root pressure coefficient comparison for different kink positions on a wing with a NACA0008 aerofoil at a 0 degree angle of attack.

lengths. The kink is ignored for calculation of the sweep angle or the taper ratio. The kink position is indicated as the spanwise position where it connects with the outer wing trailing edge, as a fraction of the semi-span length. The root aerofoil shape is kept the same and enlarged to fit the chordlength including kink.

Figure 4.10 shows a comparison between MATRICS-V and the method for different kink positions. Since the aspect ratio and sweep angle do not change, the method produces the same result for each position of the kink and therefore shows as one line. MATRICS-V does show a change for different positions of the kink. When no kink is present, the method shows the same overestimation near the leading edge that was found for the symmetric aerofoils in Section 4.2.1. When a kink is added, the overestimation occurs over the entire profile. This change on the aft part of the profile is likely caused by the reduction in effective sweep angle near the root resulting from the addition of the kink. A change in sweep has an effect of the aft part of the root effect due to thickness, as is shown in Figure 3.1.

4.2.6 COMPUTATIONAL TIME

As was explained in Section 2.2, computational times are important for a conceptual design tool. For the method developed, the computational times are given in Table 4.1 produced by a standard laptop from the year 2013. As can be seen, most of the computational time, 4.25 seconds, is used for estimating the spanwise lift. This is inevitable since the use of a VLM or equal is the minimum when estimating a reliable spanwise lift distribution.

Another 0.18 seconds is used by Xfoil to estimate the 'clean' part of the root pressure distribution, without root effect. All other parts of the method; estimating root effect due to thickness and lift, rewriting aerofoils, calculating geometry, interpolating between data, is done in only 0.36 seconds.

These final two values are of importance when the method is used for optimisation, such as the one shown in Chapter 5. For this optimisation, the spanwise lift distribution is kept the same. Therefore, the spanwise lift and the outboard (target) pressure distribution do not need recalculation every iteration. Therefore, only one Xfoil run and the other computations of the method have to be run each iteration.

Task	**Time**
AVL (spanwise lift)	4.25 sec
Xfoil (root chordwise pressure)	0.18 sec
Other	0.36 sec

Table 4.1: List of computational times for different parts of the method.

5

WING ROOT OPTIMISATION

With the method developed in Chapter 4, it is possible to estimate the pressure distribution over the root section of a wing of any geometry. This chapter uses the method to develop a method for designing a root aerofoil that produces straight isobars along the wing span. Section 5.1 explains the method in detail. The results of the method are shown and discussed in Section 5.2. In Section 5.3 the validity of the results is investigated.

5.1 METHOD

Figure 5.1 shows a schematic of the method developed for optimisation of the wing root profile. It uses the method for estimating the root pressure distribution developed in Chapter 4. This part of the method is shown in the centre of Figure 5.1.

The initial phase of the optimisation is similar to that of the method for determining the root pressure distribution. The first step is to determine the spanwise lift coefficients. The difference with the aforementioned method is that the root aerofoil will be changed in later stages. The spanwise lift coefficients, however, will be determined using the outboard aerofoil placed at the root. The section lift coefficients determined this way will be used for the remainder of the method. The decision to use the outboard aerofoil for determining the root section lift coefficient has a number of reasons. When designing an aeroplane, there can be multiple effects determining the root section lift coefficient. For this method, however, the main interest is not designing a specific aeroplane, but designing a general method for wing root design. For this reason the choice is made to make no design alterations to the root section lift coefficient. Moreover, this way the 'pure' effect of changing the aerofoil can be observed, because it can be compared to a wing with the same (outboard) aerofoil placed along the entire span.

With the spanwise lift coefficients determined, the pressure distribution on the outboard section can be estimated. The outboard section is located at the centre of the semi-span wing, halfway between the tip and the root, as shown in Figure 2.1. It is assumed that at this position the flow is undisturbed by the root and tip effects, which are explained in Section 2.3. Therefore, the pressure distribution can be estimated by using only the panel method at the local section lift coefficient. This process is described in more detail in Section 5.1.1. The estimated outboard pressure distribution is set as the target pressure distribution for the optimisation of the root profile. By doing this, the isobars are straightened as described in Section 2.4. Since there is a difference in section lift coefficient, the optimised root section will never be able to have exactly the same pressure distribution as that of the outboard section. The implications of this will be explained in Section 5.2.

Now that the target pressure distribution is set, the optimisation can be initiated to find the optimal root aerofoil. For starting the optimisation, an initial 'guess' aerofoil has to be created. In order to keep the number of design variables within reasonable limits, Class-Shape function Transformation (CST) parameters are used to describe the aerofoil shape. This is shown in Section 5.1.2. They are converted to x- and z-coordinates for use with the method as demonstrated in Section 5.1.3. With the aerofoil set, the method for determining the root pressure distribution is executed in the same way it was done in Chapter 4.

The results of the root pressure distribution estimation are compared with the estimated outboard pressure distribution, shown in Section 5.1.4. The difference between the two determines the error for the opti-

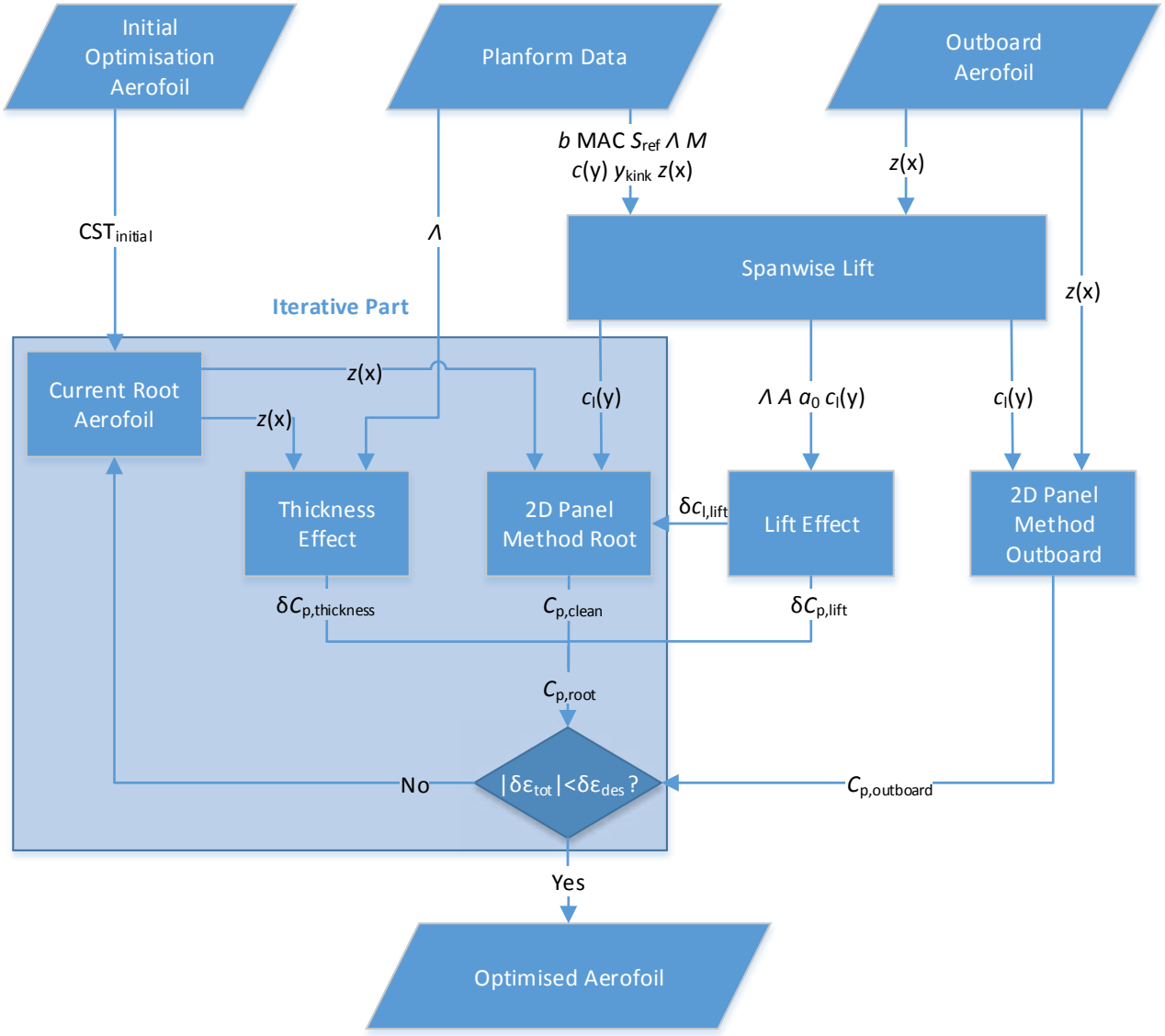

Figure 5.1: Schematic of the method for optimising the root aerofoil.

misation. With the error at the initial position known the optimisation will go back to the root aerofoil and choose new CST parameters. This results in a different aerofoil shape, for which a new root pressure distribution is determined. The root effect due to lift does not need to be determined again because it is only dependent on the planform and lift coefficient, which do not change. The second aerofoil will have a different error when compared to the outboard pressure distribution. The optimisation routine will continue to use this difference to improve the design until an optimum is found. The final result is an optimised root aerofoil with a pressure distribution similar to the outboard pressure distribution as shown in Section 5.1.5.

5.1.1 2D PANEL METHOD OUTBOARD

The *2D Panel Method Outboard* module determines the pressure on the outboard part of the wing. As is explained in Section 2.3, the outboard part of the wing is assumed to be unaffected by the root and tip effects. The pressure distribution over this section is determined by using Xfoil. The outboard section lift coefficient determined by the *Spanwise Lift* module is used. The implementation of Xfoil is similar to the method explained in Section 4.1.6. The resulting outboard pressure distribution is used by the *Compare Cp* module as the target pressure distribution for the optimisation of the root profile.

5.1.2 INITIAL OPTIMISATION AEROFOIL

For the design of the aerofoil, use is made of CST parametrisation. CST parametrisation can describe an aerofoil with a reduced number of variables compared to x- and z-coordinates, as will be explained below.

The optimisation needs a starting point from which it can start to determine the direction of the optimum design. It is important that the starting point results in a valid root pressure distribution, otherwise the optimisation cannot start. Because it needs to be valid for all wing shapes and outboard aerofoils, a very generic aerofoil is chosen. Another obvious choice would have been to use the outboard aerofoil as an initial estimate for the root aerofoil. However, since the optimisation uses CST parameters, these parameters would have to be determined for the outboard aerofoil first. This would require an inverse method and therefore an optimisation. This would take considerable computational time, which should be avoided during conceptual design. Since using the generic aerofoil as a starting point turns out not to have an effect on the final optimised aerofoil, this option is preferred.

CST PARAMETRISATION

Class-Shape function Transformation parametrisatoin is a method for describing two dimensional surface of an aerofoil with a reduced number of variables. It is based on use of the Bézier curve, but is extended with a class function. Bézier curves are based on the Berstein polynomial and can describe a curve based on a small number of variables. By adding the class function term, certain boundaries are set, which categorise the resulting shapes. In the case of CST parametrisation, this allows control of the leading edge thickness, trailing edge boattail angle and and closure to a specified aft thickness. CST parametrisation was developed by Brenda Kulfan of the Boeing Commercial Airplane Group. Besides application to two dimensional aerofoils, it can also be applied to a number of three-dimensional (aerodynamic) shapes [16].

The use of CST parametrisation greatly reduces computational time since the optimisation can work with a lower number of variables. It reduces flexibility in aerofoil design, because it can only use smooth curves. Aerofoils do, however, have smooth curves by nature. Therefore, the benefits of increased computational time outweigh the negative effect of reduced design flexibility.

5.1.3 CURRENT ROOT AEROFOIL

The *Current Root Aerofoil* module holds the current aerofoil for evaluation by the optimisation. It starts off with the initial 'guess' aerofoil supplied by the *Initial Optimisation Aerofoil*. Subsequent aerofoils are found by changing each CST coefficient separately, thereby determining the 'direction' in which the optimum design can be found.

5.1.4 ERROR FUNCTION

The error function compares the pressure distributions of the outboard and the root section, as part of the optimisation. The outboard pressure distribution comes from the *Panel Method Outboard* module and is fixed during the optimisation. The root pressure distribution comes from the method for determining the root pressure distribution, as described in Chapter 4. This result changes every iteration, because the change in root aerofoil results in a change in pressure distribution. The error at each point is defined as the difference

in pressure coefficient between the outboard (target) and the current root section. The error function is given by:

$$\epsilon_{\text{tot}} = \sum_{i=1}^{n} \left(\epsilon_{i,\,\text{upper}} + \epsilon_{i,\,\text{lower}} \right) \tag{5.1}$$

in which ϵ_{tot} represents the total error, ϵ_i the error at position i and n the total number of chordwise points. At each point the error of both the upper and the lower surface are taken. As can be seen they have equal weights in the estimation of the error.

As stated earlier, the optimisation routine finds the 'direction' of the optimum design by changing the CST parameters one at a time. This will show which parameters result in the biggest reduction in the total error, ϵ_{tot}. When the change in total error between iterations becomes lower that the desired value, $\delta\epsilon_{\text{des}}$, the optimisation has reached its optimum.

5.1.5 OPTIMISED AEROFOIL

The *Optimised Aerofoil* module is the final result of the optimisation. This aerofoil, when analysed by the method described in Chapter 4, produces a pressure distribution that is as close as possible to that of the outboard pressure distribution. Examples of optimised aerofoils are given in the next section, Section 5.2.

5.2 RESULTS

The method for optimising the wing root aerofoil has been shown in Section 5.1. This section shows the results of this method. In order to best explain the results of the optimisation method, first, an example is given in Section 5.2.1. Section 5.2.2 shows the influence of a number of design variables on the optimised root aerofoils. Since modern transonic transport aeroplanes use typical transonic aerofoils, the compatibility of the method with these aerofoils is investigated in Section 5.2.3. Finally, in Section 5.2.4, the computational time used by the method investigated.

5.2.1 EXAMPLE RESULT

Figure 5.2 shows the results of an optimisation of the root aerofoil of a 30 degree, aft swept, untapered wing with a NACA0008 aerofoil at a 6 degree angle of attack. The top of Figure 5.2 shows the original aerofoil, indicated by the dash-dotted line, and the optimised aerofoil, indicated by the solid line. The original aerofoil, which in this case is a NACA0008, is placed on the entire wing for the spanwise lift distribution. The outboard pressure distribution is estimated and used as a target for the optimisation. The outboard (target) pressure distribution is indicated in the figure by the dashed line. The original (NACA0008) root pressure distribution, indicated by the dash-dotted line, is only given to show the changes made by the optimisation. It does not play a part in the optimisation. The solid line shows the final, optimised pressure distribution over the root aerofoil.

5.2.2 INFLUENCE OF SWEEP, ANGLE OF ATTACK AND CAMBER

By showing the example in Section 5.2.1, the basics principles of the optimisation results are clear. Now, an investigation into the influences of an number of different design parameters can be made.

Figure 5.3 shows the most simple cases possible. This is an untapered wing with a NACA0008 aerofoil on the outboard section. Because the angle of attack is zero and the aerofoil is symmetrical, there is no lift. Therefore, the effect shown in the figure is only that of the root effect due to thickness. In Figure 5.3 the wing sweep angle is varied. At the top of the picture the wing is swept forward. Going down, sweep is increased, resulting in an aft swept wing at the bottom of the page. It can be seen that for the forward swept wing the thickness is decreased near the leading edge part and is increased near the trailing edge part, when compared to the outboard aerofoil. For the aft swept wing, the effect is the other way around.

In Figures 5.4 and 5.5 the results of optimisations are shown for an angle of attack of 3 and 6 degrees, respectively. By adding an angle of attack, the lift is no longer zero. This means that the results are influenced by both the root effect due to thickness and due to lift. The aforementioned change in thickness near the leading edge and trailing edge part can again be seen in the results. However, the results also show a clear change in camber and incidence angle. For a forward swept wing, as shown in the top of both figures, the camber shows increased positive camber. For aft swept wings the camber is increasingly negative. The incidence angle is shown to be increasingly negative for forward swept wings and positive for aft swept wings.

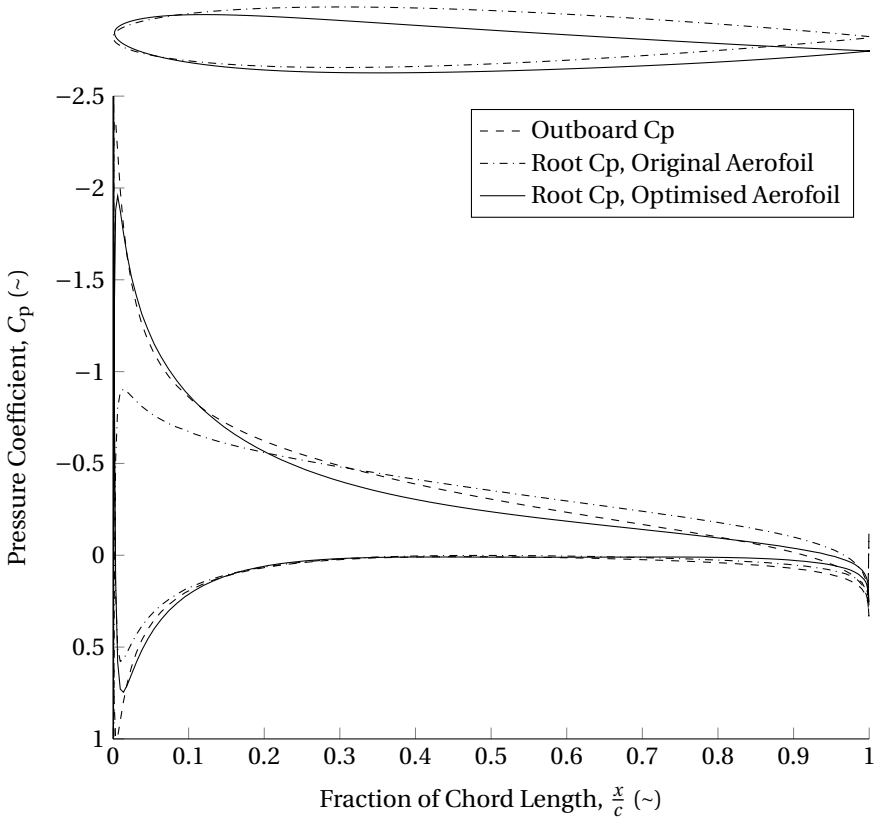

Figure 5.2: Result of root aerofoil optimisation for a wing with a NACA0008 aerofoil at a 6 degree angle of attack.

Three things can be observed when comparing results figures 5.4 and 5.5. First of all, the changes in camber and incidence angle become larger for larger angles of attack. Secondly, the position of maximum thickness does not change with increasing angle of attack. This is to be expected, since the method for estimating the root effect due to thickness is not dependent on the angle of attack. Finally, a noticeable decrease in overall thickness is observed for both positive and negative sweep angles.

Figure 5.6 shows the results of the optimisation of an untapered wing with cambered aerofoils, at a 3 degree angle of attack. From these results it can be seen that by optimising for both the upper and lower surface pressure, the general shape of the aerofoil can be maintained. In terms of camber, incidence, position of maximum thickness and overall thickness, it shows the same effects as the symmetric aerofoils shown in figures 5.4 and 5.5.

5.2.3 TYPICAL TRANSONIC AEROFOILS

The aerofoils shown up to this point have all been of the same NACA 4-digit 'family'. Modern transonic aeroplanes however, have aerofoils with a specific shape. At the top of Figure 5.7 a National Aeronautics and Space Administration (NASA)SC(2)-0412 aerofoil is shown, which is representative of these 'supercritical' aerofoils. The relatively flat upper surface of the aerofoil produces a relatively weak shock. Because of the flat top, the forward 60% of the aerofoil has negative camber, reducing the lift. To compensate the rear 30% of the aerofoil has extreme positive camber [17].

Therefore, for design of the root aerofoil of a transonic aeroplane, it is important to retain these characteristics. Because of the dependency of the wing root aerofoil design method on both the upper and lower surface pressure, this is possible. This can be seen in Figure 5.7. As can be seen, the relatively flat surface is still present, as is the characteristic positively cambered rear section. The shape has been modified by an increase in thickness in the forward part, a decrease in thickness in the aft part, a reduction of camber and an increase of the incidence angle. It is important to keep in mind that the optimisation has a simple symmetric aerofoil as a starting point. The fact that the optimisation results in an aerofoil similar to the outboard aerofoil, once more shows the ability to retain aerofoil characteristics.

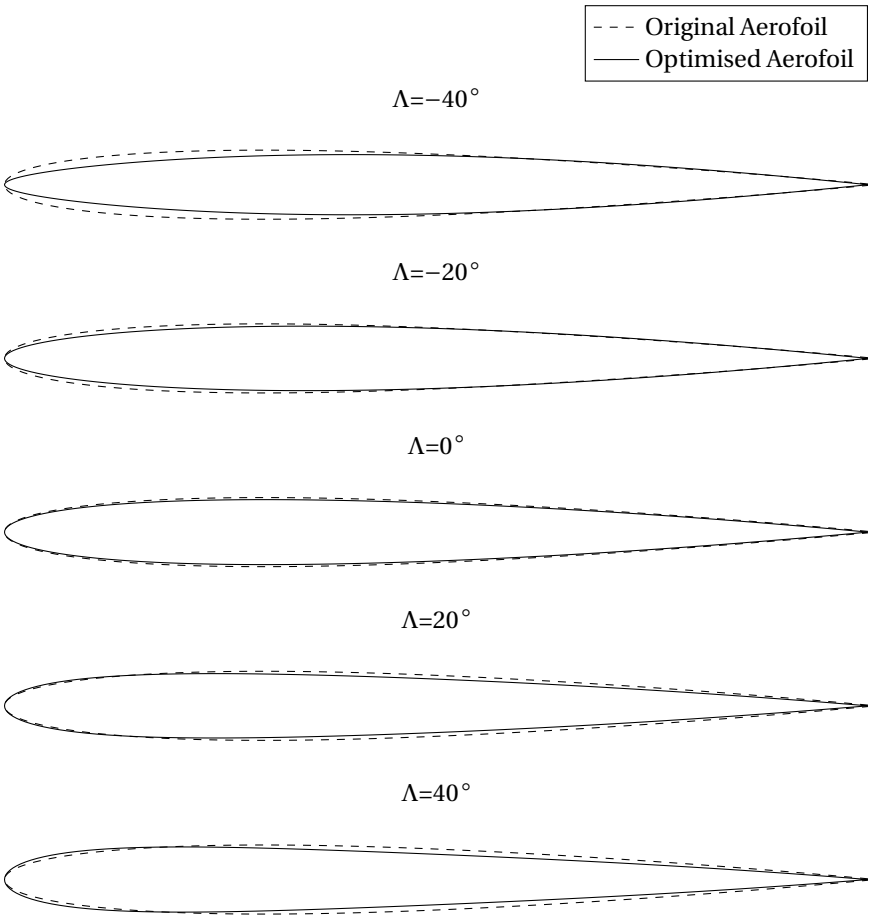

Figure 5.3: Results of root aerofoil optimisation for a wing at a 0 degree angle of attack.

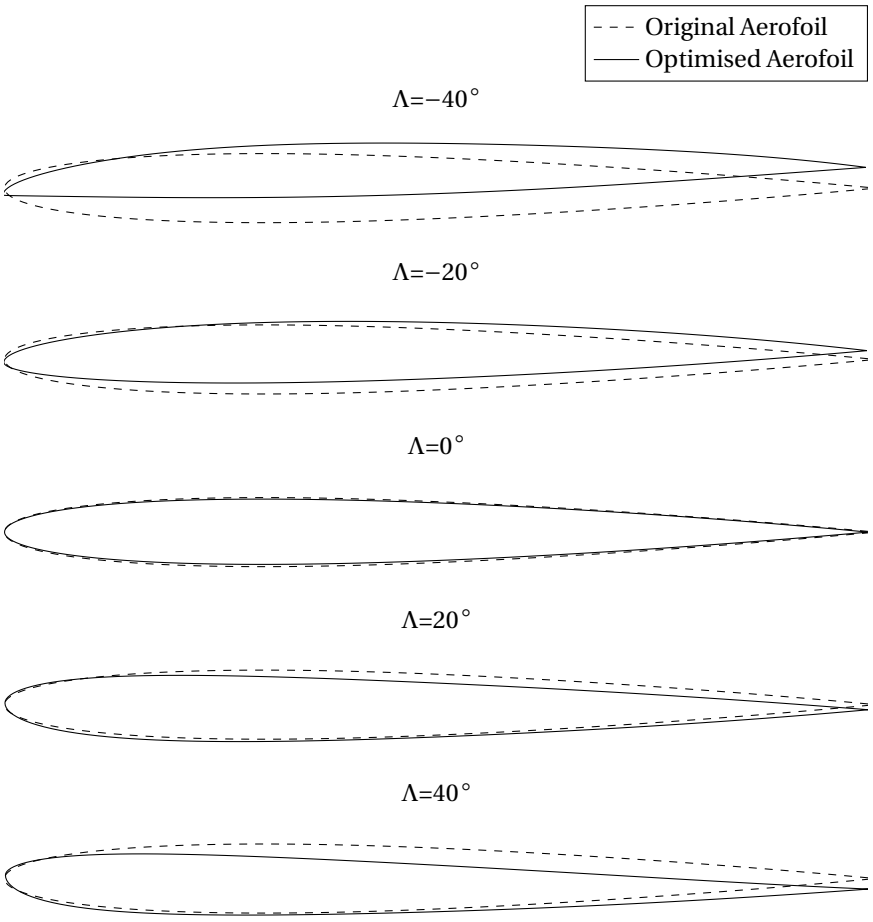

Figure 5.4: Results of root aerofoil optimisation for a wing at a 3 degree angle of attack.

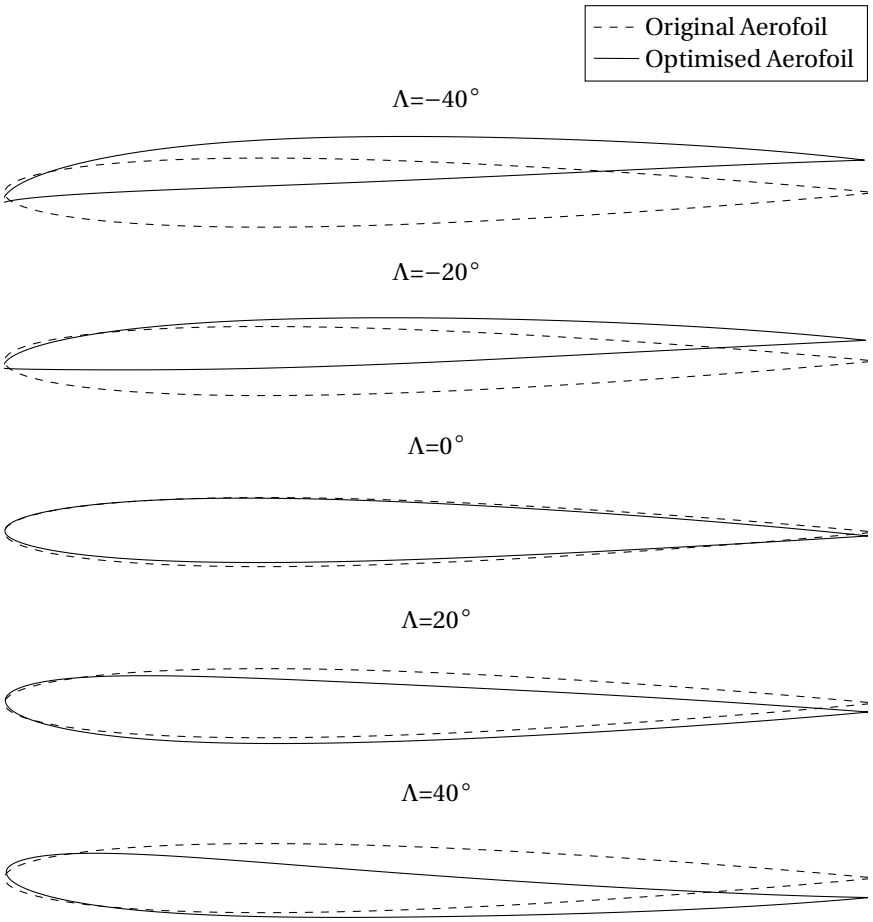

Figure 5.5: Results of root aerofoil optimisation for a wing at a 6 degree angle of attack.

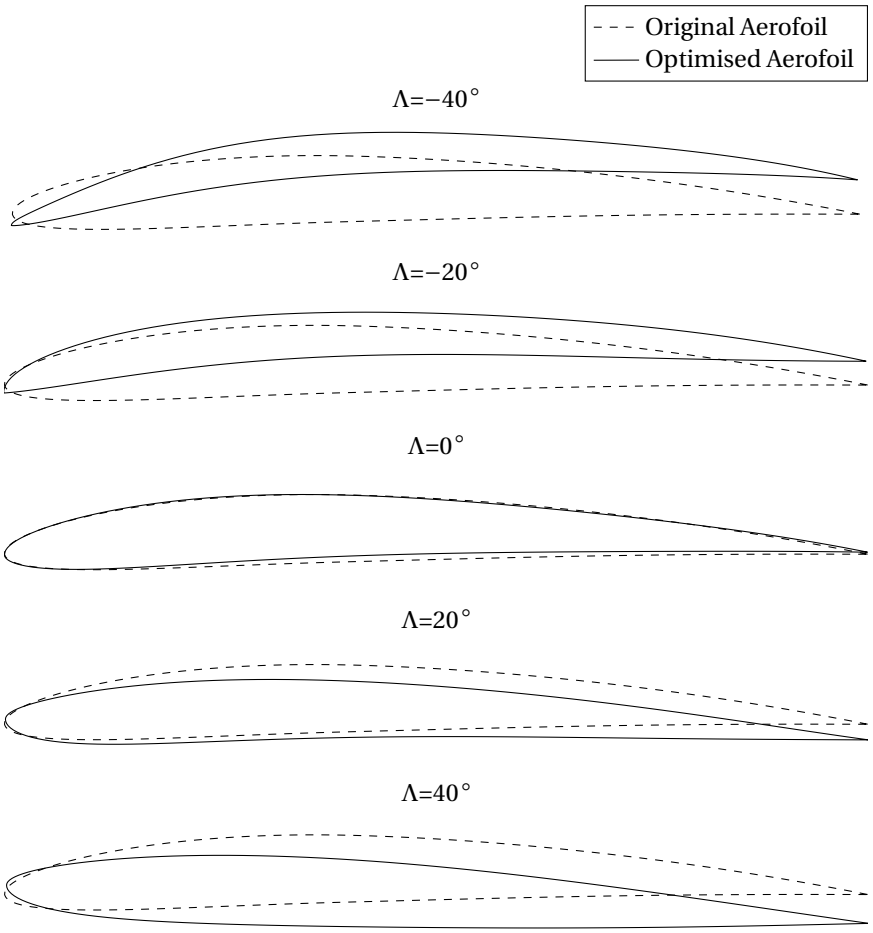

Figure 5.6: Results of root aerofoil optimisation for a wing at a 6 degree angle of attack with a cambered aerofoil.

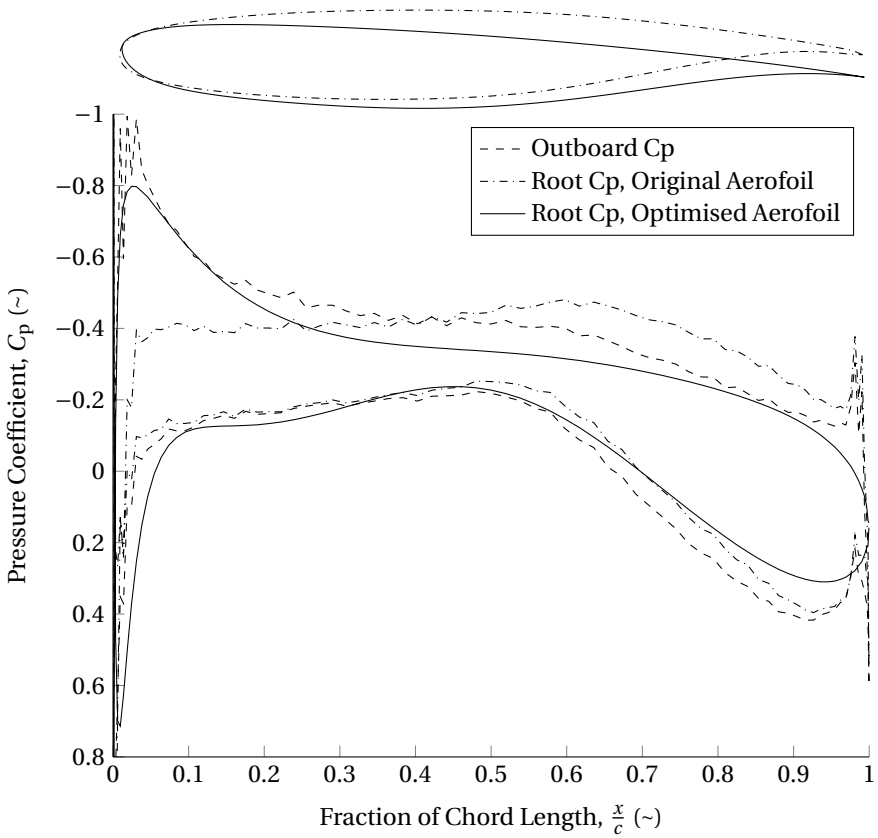

Figure 5.7: Result of root aerofoil optimisation for a wing with a NASASC(2)-0412 aerofoil at a 2 degree angle of attack.

The pressure distribution shows some erratic behaviour for the original root and outboard pressure distribution. This is due to Xfoil having trouble with the original aerofoil data. The optimised aerofoil pressure distribution, however, is smooth. This is most likely because its coordinates are based on CST parametrisation.

From the pressure distribution it can be seen that the optimisation is capable of capturing the general pressure distribution of a supercritical aerofoil. The lower surface pressure on the aft part is slightly underestimated. This may be due to the erratic behaviour of the target outboard data near the trailing edge. Also, near the centre of the aerofoil, the upper surface pressure is overestimated. This behaviour is similar to the behaviour shown in Section 5.2.1.

5.2.4 COMPUTATIONAL TIME

The computational time needed to reach an optimum design varies greatly. Some designs reach an optimum after only about 18 seconds. Some other designs keep running and never converge. This might be caused by inaccuracies in one of the models, the inability of the panel method to reach a solution for certain design points or the coupling of the methods.

It was found that, even though many designs get stuck and keep running, in almost all cases still the optimum design is reached in about 30 seconds. Therefore, the optimisation loop can be cut off after predetermined number of function evaluations, and still produce a valid design.

5.3 VERIFICATION

There is no direct way of validating the results produced by the method developed in the previous sections for wing root aerofoil optimisation. There is no process that gives the one correct answer for each case of the optimisation. However, an attempt can be made to show that the general principles of the method are valid.

A first attempt at showing the validity of the method can be made by showing that the basic principles of the method are correct. Therefore, in Chapters 3 and 4, emphasis is placed on verification of all cases using MATRICS-V. It is shown that overall the method shows good agreement with the verification data. Since

MATRICS-V shows good agreement with windtunnel tests, it is to be expected that the method also is in good agreement with these windtunnel tests. However, since this verification is indirect and based on the accuracy of a large number of different design variables, this cannot be guaranteed.

Therefore, in the following sections, the validity of the method is investigated using different methods. In Section 5.3.1 the designs resulting form the method are evaluated using the design modifications shown in Section 2.5. Section 5.3.2 analyses an optimised wing design using MATRICS-V to check whether or not straight isobars are obtained.

5.3.1 MODIFICATIONS FROM LITERATURE

In Section 2.5 a number of design modifications for obtaining straight isobars is shown. These modifications are; a change in position of maximum thickness, a change in overall thickness, a change in camber and a change in incidence angle.

In general, the behaviour of the optimisation results is in accordance with these modifications. For an aft swept wing the camber becomes more negative, the incidence angle increases and the position of the maximum thickness point moves forward. The reverse can be seen for forward swept wings.

However, it can be observed that the overall thickness of the optimised root aerofoil decreases when applying forward or aft sweep. This is not in accordance with the modifications shown in Section 2.5. It is shown that for aft swept wings the thickness should increase, while for forward swept wings the thickness should decrease. There are two effects that are the most likely causes for this.

Part of this could be caused by the difference in lift coefficient combined with the target pressure distribution. Because of the wing shape, the section lift coefficient at the root differs from that at the (target) outboard section. The section lift coefficient determines the area between the upper and lower surface pressure coefficient and therefore the distance between these lines. During the design of a wing, the upper surface of the wing is of most importance, since, because of the orientation of the profile, the upper surface has the most influence on pressure drag and M_{dd}. During design of an aft swept wing, the values of the pressure coefficient on the upper surface of the wing are lower because of the lower lift coefficient (which causes a lower difference between the upper and lower surface values). Normally, this higher pressure coefficient is countered by increasing thickness of the profile, since this decreases both the upper and lower surface pressure. However, in the method developed, the design is optimised for both the upper and lower surface pressure. Therefore, the thickness is not increased. The reverse is true for the forward swept wing, where the lift coefficient is higher. The resulting lower pressure coefficient on the upper surface is again not countered by decreasing thickness.

The actual decrease in thickness is likely caused by another effect. Most likely it is caused by the emphasis on the leading and trailing edge regions, caused by the cosine distribution of points. In an attempt to meet the low pressure values near the leading edge while maintaining the lower lift coefficient, the pressure at the centre section becomes higher than the target value, reducing the thickness of the optimised aerofoil. The optimisation of the forward swept wing also puts emphasis on the leading and trailing edge parts. Even more so near the leading edge of the upper surface because of the exponential nature of the pressure distribution at this location. Attempting to meet the higher pressure at this location likely pushes up the pressure of the rest of the upper surface. In order to meet the higher lift coefficient, the lower surface pressure also becomes higher, decreasing thickness.

Concluding, the results of the optimisation show most of the effects that are to be expected when designing a wing root aerofoil. These are; changes in camber, changes in incidence angle and changes in the position of maximum thickness. The results of the method however, do not show the expected change in overall thickness. Because of the emphasis on leading and trailing edge this may be more pronounced in the centre of the aerofoil.

5.3.2 MATRICS-V ANALYSIS

Another way of verification, that the root aerofoil design method produces the desired results can be performed using MATRICS-V. The root aerofoil design resulting from the optimisation should produce a root pressure distribution similar to that of the outboard section. By analysing this optimised design using MATRICS-V, the pressure distribution over the designed wing can be investigated. The results of this analysis are independent of any of the assumptions made during development of the method, since only the geometry is put into MATRICS-V. Since MATRICS-V has a higher level of 'fidelity' than any part of the method, as was shown in Section 3.1.2, the results should give a good estimate of the quality of the optimised design.

The method developed in this report only produces an optimised root aerofoil and its incidence angle. No

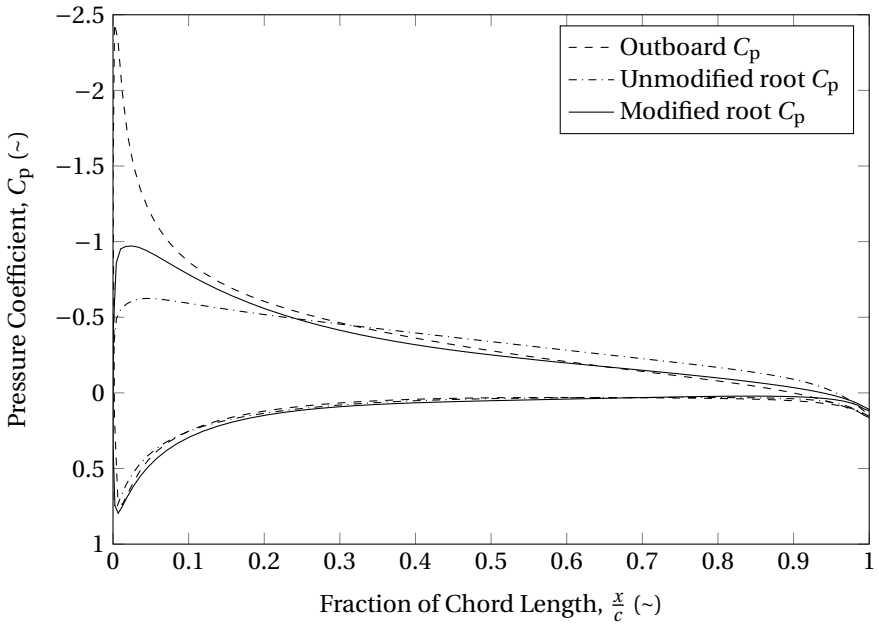

Figure 5.8: Chordwise pressure distribution of a MATRICS-V analysis of an optimised design.

assumptions were made on how to blend this design into the rest of the wing, other than that the outboard section should not be influenced. In Section 2.3, it is shown that the root aerofoil should blend into the wing at about 30% of the semi-span. Therefore, the wing analysed by MATRICS-V has the optimised aerofoil defined at the wing root. At 30% semi-span and at the tip, a NACA0008 is defined. MATRICS-V then blends the aerofoil linearly.

Together with the optimised wing, a control analysis is made using MATRICS-V with an unmodified wing with a NACA0008 aerofoil across the entire wing span. Both wings are untapered, swept aft 30 degrees and at a 6 degree angle of attack. The resulting pressure distributions are shown in Figure 5.8. The outboard pressure distribution is the same for both wings. As can be seen, the modified pressure distribution is significantly closer to the outboard pressure distribution as the pressure distribution of the unmodified aerofoil. This should result in straightening of the isobars.

The isobar distribution over upper surface of the aforementioned wings, both for the unmodified and the modified wing, are shown in Figure 5.9. The plane of symmetry for both wings is on the x-axis. The figure shows the first 8 meters of the wing with a semi-span of 20 meters. The full extend of the isobar sweep is not shown in the picture, since the underlying data in spanwise direction is only available every 2 meters. All the lines in between these spanwise stations are straight.

At a first glance, the isobar distribution hardly seems to have improved by modifying the wing root aerofoil. Only the leading edge near the plane of symmetry seem to show improved straight isobars. This does not correspond to the match in pressure distribution shown in Figure 5.8. The reason for this is the blending method used by MATRICS-V. The wing root aerofoil was blended into the rest of the wing at 30% semi-span. This corresponds to the 6 meter spanwise station in Figure 5.9. The part of the wing outboard of the 6 meter spanwise station is not influenced by the modifications. In Figure 5.10, the direction of one of the isobars on this outboard section is taken en extended towards the root. When following the isobars towards the root, it can be seen that they first move forward relative to the reference line and at some point they move aft. They end up approximately on the same extended outboard isobar.

This shows that the root aerofoil is approximately accurate for designing straight isobars, but the blending method is not. Part of the flow outboard from the root section is 'overcompensated'. This is due to the linear nature of the blending used by MATRICS-V. As can be seen in Figure 3.5 the root effect has a non-linear nature. Therefore, when blending the optimised root aerofoil into the main wing, an exponential factor like the k factor should be used.

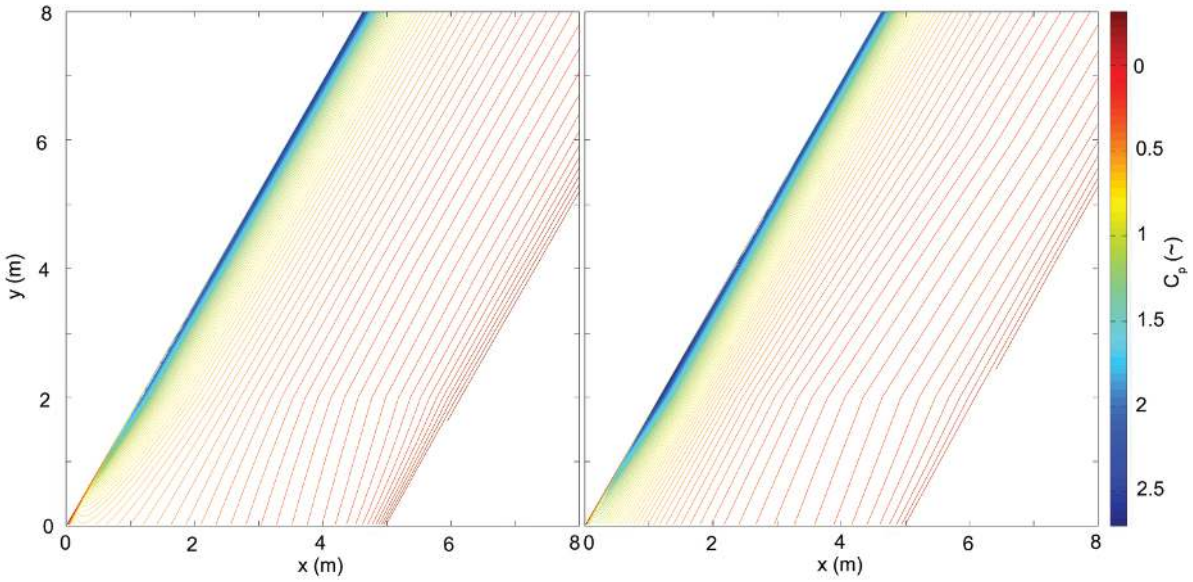

Figure 5.9: Comparison of root isobar distribution on an unmodified and a modified wing.

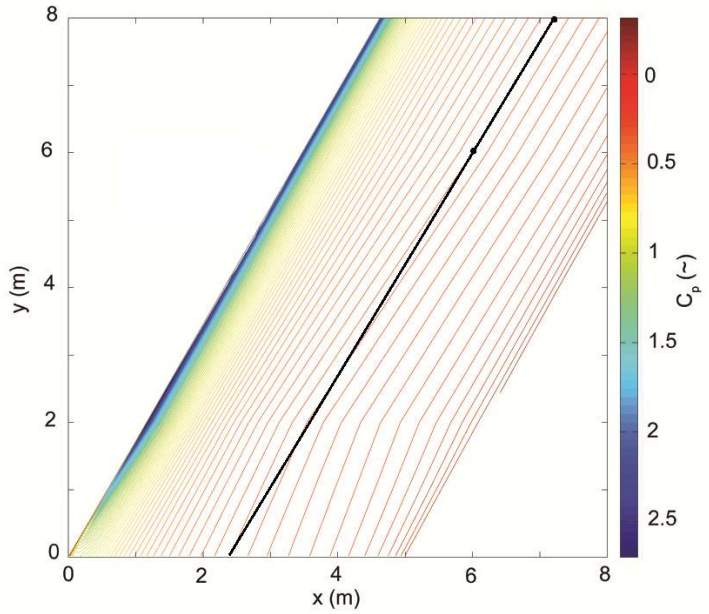

Figure 5.10: Comparison of root isobar distribution on an unmodified and a modified wing.

6

CONCLUSIONS

A method for conceptual design of the wing root aerofoil is developed. The objective of this method is to achieve a design resulting in straight isobars, using only the outboard aerofoil and basic wing geometry. Computational time is kept within 30 seconds to allow for use in iterative conceptual methods.

It is shown that the resulting root aerofoil designs have three of the four characteristic aspects observed in actual aeroplane design for straight isobars. These aspects are; change in position of maximum thickness, a change in aerofoil camber and a change in incidence angle.

The change in overall thickness, however, is not in accordance with the characteristic aspects. It shows a decrease in overall thickness for aft swept wings, while in practice the overall thickness increases with increasing sweep angle. The thickness increase observed in practice for aft swept wings is to achieve a similar upper surface pressure distribution to that of the outboard section, while compensating for the lower lift coefficient. Since the method developed in this report places equal importance on the upper and lower surface, this thickness increase is not observed.

By placing equal importance on the upper and lower surface, the method has the ability to retain the characteristic shape of the outboard aerofoil. This is of special importance when designing a wing using supercritical aerofoils. It is shown that, even though the starting point of the optimisation is a simple symmetric aerofoil, the end result still shows the characteristic shape of a supercritical aerofoil.

It is observed that almost all inputs converge to an optimal design. In some case within as less as 18 seconds. In most cases, the design optimum is reached after about 30 seconds, which is suitable for conceptual design applications.

The method is verified by analysing an optimised design using a full potential method. The results show that the root section pressure distribution is similar to that of the outboard section. To achieve straight isobars, special care must be taken with respect to blending the designed root aerofoil into the wing.

7

RECOMMENDATIONS

During the developement of the method for conceptual root aerofoil design, a lot of experience was gained. Some specific to the developed method, some more general in the field of wing root design. This chapter shows a number of recommendations that might be of interest for people who want to continue research into this subject.

- The method developed for conceptual wing root aerofoil design, has been verified by analysis at low subsonic speeds. The application of these designs, however, is at transonic speeds. It is assumed that with the increase in speed to transonic speeds, the pressures along the wing will develop in similar way at all positions on the wing. This would retain the straight isobar design. However, this has not been investigated.
- The method for wing root aerofoil design has been developed for implementation into a full aeroplane conceptual design method. It would be interesting to see the effects of this improved root aerofoil design on the scale of an entire aeroplane. Especially its effect on wing weight.
- The method for determining the root effect due to lift, is based on an old VLM developed for symmetrical aerofoils. For development of the method for conceptual design of the wing root aerofoil, camber was applied to this method, without changing the method itself. This results in inaccuracies for cambered aerofoils. Modern VLM methods, however, can cope with cambered aerofoils. It might therefore be possible to use parts of this method to improve results for cambered aerofoils.
- The method for determining the root effect due to thickness, is dependent on the wing sweep angle. When adding a wing kink to the design, the method does not calculate the change in local sweep angle near the root. This is the likely cause of the error introduced by adding a kink, shown in Section 4.2.5. By developing a way of determining the effective sweep angle for the thickness method, results including a wing kink could be improved.
- It was shown in Section 5.3.2, that using linear blending of the root aerofoil into the wing, does not result in straight isobars. Even though the root section has a similar pressure distribution to the outboard section, the intermediate points do not. In order to achieve straight isobars, an investigation could be made into a method for blending the root aerofoil into the wing. A suggested starting point for this would be the report by Bridgewater et Al. [2].
- By making a number of changes to the method, it might be possible to apply it at all spanwise positions. The method for estimating the root effect due to thickness is technically only valid for application at the root. However, since at the root the effects are opposite to those at the tip, perhaps, the method could be applied by scaling the sweep angle for the thickness method by the k factor shown in Figure 3.5. Application of the method at the wing tip itself would probably need additional modelling, since tip design is also influenced by the tip vortices.

BIBLIOGRAPHY

[1] E. Obert, *Aerodynamic Design of Transport Aircraft* (IOS Press, Nieuwe Hemweg 6b, 1013 BG Amsterdam, The Netherlands, 2009).

[2] J. Bridgewater and K. H. Wilson, *Influence of Wing Root Shaping on the Pressure Distribution of Swept-Wing Body Configurations*, Tech. Rep. ARC - C/P 1109 (Aeronautical Research Council London (England), 1969).

[3] S. Obayashi, S. Takahashi, and I. Fejtek, *Transonic wing design by inverse optimization using moga,* in *Sixth Annual Conference of the Computational Fluid Dynamics Society of Canada* (Computational Fluid Dynamics Society of Canada, 1998).

[4] E. Torenbeek, *Synthesis of Subsonic Aircraft Design* (Delft University Press, 1976).

[5] D. P. Raymer, *Aircraft Design: A Conceptual Approach* (American Insitute of Aeronautics and Astronautics, inc., 370 L'enfant Promenade, S.W., Washington, D.C. 20024, 1992).

[6] R. Elmendorp, R. Vos, and G. L. Rocca, *A conceptual design and analysis method for conventional and unconventional airplanes,* in *29th Congress of the International Council of the Aeronautical Sciences* (Delft University of Technology, 2014).

[7] J. Roskam, *Airplane Design; Part I: Preliminary Sizing of Airplanes* (Roskam Aviation and Engineering Company, Rt4, Box 274, Ottawa, Kansas, 66067, 1985).

[8] D. Küchemann and J. Weber, *The Subsonic Flow Past Swept Wings at Zero Lift Without and With Body*, Tech. Rep. ARC - R/M 2908 (Aeronautical Research Council London (England), 1956).

[9] H. Multhopp, *Methods for Calculating the Lift Distribution of Wings (Subsonic Lifting Surface Theory)*, Tech. Rep. Aero 2353 (Royal Aircraft Estabishment, Farnborough (England), 1950).

[10] J. Mariens, *Wing Shape Multidisciplinary Design Optimization*, Master's thesis, Delft University of Technology (2012).

[11] A. Elham, *Weight Indexing for Multidisciplinary Design Optimization of Lifting Surfaces*, Ph.D. thesis, Delft University of Technology (2013).

[12] A. van der Wees, J. van Muijden, and J. van der Vooren, *A fast and robust viscous-inviscid interaction solver for transonic flow about wing/body configurations on the basis of full potential theory,* in *24th AIAA Fluid Dynamics Conference* (The American Institute of Aeronautics and Astronautics, 2009).

[13] D. Küchemann, *A Simple Method of Calculating the Spanwise and Chordwise Loadings on Thin Swept Wings at any Given Aspect Ratio at Subsonic Speeds*, Tech. Rep. ARC - R/M 2935 (Aeronautical Research Council London (England), 1952).

[14] M. Drela and H. Youngren, *AVL User Primer*, 3rd ed. (2010).

[15] M. Drela, *XFOIL: An Analysis and Design System for Low Reynolds Number Airfoils*, Tech. Rep. (Massachusetts Insitute of Technology, 1989).

[16] B. M. Kulfan, *A universal parametric geometry representation method - "cst",* in *45th AIAA Aerospace Sciences Meeting and Exhibit* (The American Institute of Aeronautics and Astronautics, 2007).

[17] J. D. Anderson, Jr., *Fundamentals of Aerodynamics* (McGraw-Hill, 2007).